NASA TECHNICAL MEMORANDUM

NASA TM X-1571

NASA TM X-1571

STUDY OF UNDEREXPANDED EXHAUST JETS OF AN X-15 AIRPLANE MODEL AND ATTACHED RAMJET ENGINE SIMULATOR AT MACH 6.86

by Earl H. Andrews, Jr., and R. Clayton Rogers

Langley Research Center

Langley Station, Hampton, Va.

NATIONAL AERONAUTICS AND SPACE ADMINISTRATION • WASHINGTON, D. C. • MAY 1968

NASA TM X-1571

STUDY OF UNDEREXPANDED EXHAUST JETS OF AN X-15 AIRPLANE MODEL AND ATTACHED RAMJET ENGINE SIMULATOR AT MACH 6.86

By Earl H. Andrews, Jr., and R. Clayton Rogers

Langley Research Center
Langley Station, Hampton, Va.

NATIONAL AERONAUTICS AND SPACE ADMINISTRATION

For sale by the Clearinghouse for Federal Scientific and Technical Information
Springfield, Virginia 22151 – CFSTI price $3.00

STUDY OF UNDEREXPANDED EXHAUST JETS OF AN X-15 AIRPLANE MODEL AND ATTACHED RAMJET ENGINE SIMULATOR AT MACH 6.86

By Earl H. Andrews, Jr., and R. Clayton Rogers
Langley Research Center

SUMMARY

An investigation has been conducted using a 0.02-scale model of the X-15 airplane with a ramjet engine simulator attached to the underside of its afterbody. The investigation was initiated to approximate the effects of the ramjet exhaust plume upon the external pressures of a nozzle extension of an X-15 engine. The nozzle extension was tested with and without a simulated manifold designed to collect and to eject overboard auxiliary gases from the X-15 airplane. Tests were conducted at a free-stream Mach number of 6.86, at a stagnation temperature of about 631° K, at total pressures ranging from 5 to 17.5 atmospheres, and with the model positioned at angles of attack of 0° and 3°. Unheated air was exhausted from the nozzle of the X-15 engine and the nozzle of the attached ramjet engine simulator at total-pressure ranges of 0 to 100 atmospheres and 0 to 5 atmospheres, respectively.

The presence of the ramjet and its pylon tended to cause the afterbody surface pressures on the X-15 airplane to remain constant and not be affected by underexpanded exhaust plumes of the X-15 and ramjet nozzles. The pressure-measuring station nearest the base of the X-15 afterbody did, however, experience an increase as the exit-to-ambient static-pressure ratio of the X-15 nozzle increased.

Static-pressure measurements and schlieren photographs indicated that the ramjet nozzle exhaust plume initially impinged upon the nonblowing X-15 nozzle extension at very small ratios of ramjet nozzle-exit pressure to ambient static pressure of 8 and 12 for angles of attack of 0° and 3°, respectively. Upward forces on the X-15 nozzle extension caused by operation of the ramjet nozzle were approximated; the forces without the manifold ring were greater than those with the ring.

INTRODUCTION

Ramjet engines are of general interest because of the high specific impulse and relative mechanical simplicity. Performance calculations for the Mach 3 to 7 range

indicate that fuel-specific-impulse values for subsonic combustion ramjets may be six or more times greater than those for chemical rockets (ref. 1). Dissociation losses and high internal static pressures of subsonic combustion ramjets result in performance degradation above about Mach 7. Recent investigations have indicated that by employing supersonic combustion, these problems may be alleviated, and high values of fuel specific impulse may still be achieved. As a consequence, many phases of research are being conducted in relation to supersonic combustion. The NASA Hypersonic Research Engine Project has as an objective the development of a hydrogen-fueled research ramjet engine which has both subsonic and supersonic combustion capability for operation between Mach 3 and 8. It has been proposed to conduct flight tests of the ramjet engine by attaching it to the underside of the afterbody of the X-15-2 airplane. With this arrangement, the nozzles of the ramjet and the X-15-2 will be in proximity to each other. One possible problem area, therefore, concerns the impingement of the underexpanded ramjet exhaust on adjacent surfaces such as the X-15-2 engine nozzle. Another area of concern is the effect of the interaction between the adjacent nozzle exhausts upon the afterbody surface pressures.

Since an understanding of the impingement and interference problems is of interest, the investigation reported herein was conducted on a 0.02-scale model of the X-15 airplane with a simulated ramjet engine attached to the underside of the afterbody. To determine the effects of impingement of the ramjet exhaust on the simulated X-15 nozzle, pressure distributions were obtained on the exterior of the nozzle. Static pressures on the underside of the X-15 afterbody were also measured. These tests were performed at a free-stream Mach number of 6.86, over Reynolds numbers per meter ranging from 2.13×10^6 to 7.40×10^6, and with the model positioned at angles of attack of 0^o and 3^o.

SYMBOLS

d	diameter, centimeters
M	Mach number
p	pressure, atmospheres $\left(1 \text{ atmosphere equals } 101.325 \text{ kN/m}^2\right)$
$p_{j,ram}/p_\infty$	ramjet pressure ratio (ratio of ramjet nozzle-exit pressure to ambient static pressure)
$p_{j,X-15}/p_\infty$	X-15 static-pressure ratio or exit-to-ambient static-pressure ratio (ratio of nozzle-exit static pressure to ambient static pressure)

R	Reynolds number per meter
x	distance downstream of fuselage base, centimeters
x_n	length of X-15 nozzle extension, centimeters
α	vehicle angle of attack, degrees
γ	ratio of specific heats
δ	angle of oblique shock wave, degrees
δ_{sep}	angle defining boundary-layer separation on X-15 afterbody assumed in calculations of ϕ in presence of free-stream flow, degrees
θ_n	half-angle of nozzle expansion, degrees
ϕ	initial turning angle of underexpanded exhaust gas at nozzle lip, degrees

Subscripts:

j	nozzle exit
ram	ramjet
th	throat
t	total or stagnation
∞	free-stream conditions ahead of shocks; ambient
X-15	X-15 model or full-scale prototype
1 to 8	locations of surface pressure orifices

APPARATUS AND PROCEDURE

Wind Tunnel and Tests

The investigation reported herein was conducted in the Langley 11-inch hypersonic tunnel at a free-stream Mach number of 6.86, at an approximate stagnation temperature of 631° K, over Reynolds numbers per meter ranging from 2.13×10^6 to 7.40×10^6, free-stream total pressures from 5 to 17.5 atmospheres, and with the model positioned at angles of attack of 0° and 3°. At these tunnel conditions the boundary layer over the model is predominantly laminar. Attempts made to trip the boundary later in the investigation of reference 2 were unsuccessful. Maximum tunnel operating time was approximately 60 seconds. The variation in Mach number after the first 10 seconds of running time was about 1 percent. The stagnation temperature of 631° K was sufficient to avoid air liquefaction during the test. Further details of the tunnel facility may be found in references 2 and 3.

Models

The photographs of figure 1 show the 0.02-scale model of the X-15 airplane with the ramjet engine simulator in place on the underside of the afterbody. The model is shown with the extended nozzle which has an exit Mach number of 4.1.

X-15 model.- Sketches showing some construction details and pertinent dimensions of the X-15 model are shown in figure 2. The fuselage is a 0.02-scale model which nearly duplicates the original X-15 prototype but not the X-15-2 airplane of particular interest; the difference between the two was small and considered to be unimportant. A scale model of the X-15-2 airplane would have been 1.47 centimeters longer than the model used, with additional length being of constant-area cross section. The model did not have vertical or horizontal fins and the wings were replaced with an 8.75-percent-thick strut which supported the model on the left side from the tunnel side wall. When the model was positioned at an angle of attack of 0°, the model axis was coincident with the tunnel axis. Pressure-measuring tubes and the air-supply tubes were contained in the wing strut. Symmetrical airflow on either side of the fuselage was obtained by extending the wing strut from the right side of the fuselage.

X-15 nozzles.- Figure 3 is a sketch of the conical convergent-divergent nozzles which were inserted into the fuselage base of the X-15 model. The nozzles had semi-divergence angles of 20° and 15° and exit Mach numbers (based on area ratios for $\gamma = 1.4$) of 3.4 and 4.1, respectively. The nozzle with the exit Mach number of 3.4 represents the original X-15 nozzle and is referred to herein as nozzle A. The nozzle with the exit Mach number of 4.1, referred to herein as nozzle B, represents a nozzle extension which is required to approach a Mach 8 flight speed. Nozzle B (fig. 3(b)) was tested

with and without a peripheral ring that simulated a manifold for dumping the gases of an auxiliary hydrogen-peroxide pump. The nozzle without the ring was designated B1 and the nozzle with the ring was designated B2.

Ramjet engine simulator.- The engine model which exhausted air to simulate the exhaust plume of a hypersonic ramjet engine is shown in the detailed sketch of figure 4. The engine is shown with the support pylon in place. Although a through-flow model would have been more desirable from a flow simulation standpoint, the small scale of the model required a simplified design. The design employed was a circular cylinder with the forebody cut at a wedge angle of 13° to direct flow disturbances downward and to allow essentially undisturbed flow along the top of the engine. If the inlet section of the engine had been fully simulated, the external flow around the cowling would have contained some compression and expansion waves. Air was supplied to the engine as shown in the figure and exhausted through a convergent-divergent conical nozzle having an exit Mach number of 3.3 and a semidivergence angle of 15°.

The location of the ramjet engine simulator with respect to the X-15 model is shown in figure 1 and in the side-view sketch of figure 2. The ramjet nozzle exit plane was coincident with the X-15 model base. The ramjet center line was 2.02 ramjet-exit diameters (shown in fig. 4 as 2.617 cm) below the X-15 nozzle center line; the ramjet exit was 1.65 ramjet-exit diameters (shown in fig. 2 as 2.143 cm) upstream of the longer (nozzle B) X-15 nozzle exit. The pylon (fig. 4) had an included wedge angle of 12° and a leading-edge sweep angle of 60°. The exact flight configuration with respect to the position of the ramjet engine relative to the X-15 will not be determined until the late stages of the project; however, it will probably be different from that used in the current investigation. Since the current preliminary investigation was designed to identify problem areas, use of the exact configuration was not considered to be important.

Air Supply

Air supplied to the nozzles had a total pressure of approximately 120 atmospheres at near atmospheric temperature and was dried to a dewpoint of approximately 233° K. The air supply was throttled to obtain total pressures that ranged from approximately 0 to 100 atmospheres for the X-15 nozzle and 0 to 5 atmospheres for the ramjet engine simulator nozzle. The Langley 11-inch hypersonic tunnel had free-stream stagnation pressures of 5, 10, and 17.5 atmospheres so that the resulting exit-to-ambient static-pressure ratios of the X-15 and ramjet engine nozzles were as follows for a value of γ of 1.4:

$p_{t,\infty}$, atm	R_∞ per meter	$p_{j,X\text{-}15}/p_\infty$ for –		$p_{j,ram}/p_\infty$ for ramjet nozzle ($M_j = 3.3$)
		Nozzle A ($M_j = 3.4$)	Nozzle B ($M_j = 4.1$)	
5	2.13×10^6	0 to 1102	0 to 420	0 to 63.75
10	4.25	0 to 551	0 to 210	0 to 31.88
17.5	7.40	0 to 315	0 to 120	0 to 18.20

Instrumentation

Three static orifices (0.102 centimeter in diameter) were located longitudinally on the underside of the X-15 afterbody, as shown in figure 2. For some of the tests, five static orifices were installed on the external surface of nozzle B. These orifices were located as shown in figure 3. Air supply to the X-15 nozzle was shut off during the tests with the nozzle external surface pressure orifices installed since the orifice tubing leads were routed through the nozzle throat and the air-supply tubes in the wing strut. Air-supply pressures for the X-15 and ramjet nozzles were measured in small offset chambers ahead of the stagnation chambers as shown in figures 2 and 4. Pressure transducers employed in this investigation had the following pressure-measurement ranges:

For $p_{t,X\text{-}15}$	0 to 133 atm
For $p_{t,\infty}$	0 to 40 atm
For $p_{t,ram}$	0 to 10 atm
For surface static pressure	0 to 0.07 atm

All pressure measurements were continuously recorded on an oscillograph recorder.

The schlieren photographs were obtained by use of an off-axis, single-pass, two-mirror, schlieren system utilizing a mercury vapor light source. Schlieren photographs were recorded on standard panchromatic film exposed for approximately 1/150 second.

SIMULATION OF INITIAL EXHAUST-PLUME SHAPE

The rocket engine of the X-15-2 airplane has a chamber pressure of 40.8 atmospheres and a ratio of specific heats equal to 1.2. For these conditions, the variations with altitude of the exit-to-ambient static-pressure ratio for the original nozzle (nozzle A, $M_j = 3.4$) and for the extended nozzle (nozzle B, $M_j = 4.1$) are shown in figure 5. These variations were obtained by using the tables of references 4 and 5.

One of the objectives of this investigation was to obtain a reasonable simulation of the exhaust-plume shape immediately downstream of the two nozzles of the X-15 model.

Since air, γ of 1.4, was used as the exhaust medium and the actual nozzle exhaust gases have a value of γ of 1.2, it was necessary to test at equivalent static-pressure ratios for γ of 1.4 so that the initial turning of the exhaust plume could be reasonably simulated. Therefore, the initial turning of the exhaust plumes of the two different nozzles was calculated for the two ratios of specific heats as a function of exit-to-ambient static-pressure ratios. These results are presented in figure 6 for nozzles A and B, whose nozzle gases are expanding into a free-stream flow, $M_\infty = 6.86$. The initial turning of the expanding gases was obtained in the manner presented in reference 6; that is, it was assumed that the fuselage boundary layer separated at a constant angle ($\delta_{sep} = 30^o$, as suggested by ref. 6) and formed a weak oblique shock upstream of the nozzle exit. (See sketch at top of fig. 6.) Two-dimensional oblique-shock and expansion relations were then used to compute stream conditions.

Similarly, calculations of the initial turning angle at the nozzle exit of the simulated ramjet engine were performed for ramjet operation over the X-15-2 test flight envelope. However, free-stream flow conditions were established by assuming that the boundary layer did not spearate from the engine nacelle. (Calculations were simplified by use of ref. 7.) Preliminary results indicated that the initial turning angle of a typical full-scale ramjet varied only slightly over the proposed X-15-2 flight envelope and had an average value of approximately 17^o for the appropriate values of γ and a θ_n of 15^o. The variations were small because the chamber pressure does not remain constant as altitude and/or flight Mach number vary. Since the total pressure of the ramjet engine simulator could be varied, exhaust-turning-angle calculations were performed for the simulator for various exit-to-ambient static-pressure ratios. The results of these calculations are presented in figure 7. The near-constant initial turning angle of 17^o for the typical ramjet is shown in figure 7 to be simulated at an approximate exit-to-ambient static-pressure ratio of 10.8 for a γ of 1.4 and θ_n of 15^o.

RESULTS AND DISCUSSION

Factors Influencing Afterbody Surface Pressures

Surface pressures on the X-15 model afterbody were measured to determine the influence of various factors on the pressures. Factors investigated were the presence of the ramjet and pylon and the effect of the combined X-15 and ramjet underexpanded exhaust gases. The X-15 model was positioned at angles of attack of 0^o and 3^o and was tested with two different exit nozzles. Results are presented in figures 8 to 11. (The pressure subscripts correspond to the orifice numbers indicated in fig. 2.) Results shown in these figures for the cases corresponding to the ramjet engine simulator attached to the model are presented for the ramjet engine simulator operating at $p_{j,ram}/p_\infty \approx 10$. Curves presented for nozzle B represent either nozzle B1 or B2.

Effect of attached ramjet engine simulator and pylon.- The effect of the ramjet engine simulator and pylon on the measured afterbody surface pressures of the X-15 model is shown in figures 8 and 10 by the comparison between the solid and open square symbols. The curves present results of tests on the extended nozzle (nozzle B) of the X-15 model at a free-stream total pressure of 10 atmospheres. The solid symbols represent the X-15 model without ramjet engine simulator and pylon.

Data for the model at an angle of attack of 0° are presented in figure 8. Curves for the most rearward orifice (orifice 1) show similar trends of pressure-ratio increase with increasing X-15 nozzle-exit pressure; thus, the presence of the ramjet and pylon has little effect upon the surface pressures at this location. Curves for the two upstream positions (orifices 2 and 3), however, indicate that the presence of the ramjet and pylon did have an effect. When the ramjet and pylon were not present, the surface pressures increased rapidly with increasing X-15 static-pressure ratios and thereby indicated, as did reference 2, that there is a considerable separated-flow region over the X-15 model afterbody. However, with the ramjet engine simulator attached, the pressures measured by orifices 2 and 3 remained constant. These constant pressures could have resulted from several sources: (1) flow separation on the afterbody induced by the shock off the pylon, (2) pressure rise across the shock off the pylon, or (3) a combination of the previous sources. The lack of detailed pressure distributions and flow visualization studies along with the complexity of the flow field in the afterbody region precludes a more thorough analysis. The curves presented in figures 8 and 10 indicate that the influence of the ramjet and pylon upon the afterbody surface pressures was less pronounced for the model positioned at an angle of attack of 3° than for the model positioned at an angle of attack of 0°.

Nozzle exhaust gas expansion.- With the ramjet and pylon installed, figures 8 and 10 indicate that the pressures at the location of orifice 1 are the only ones affected by changes in the static-pressure ratio of the X-15 nozzle. This effect was smaller at an angle of attack of 3° than at an angle of attack of 0°. The schlieren photographs of figure 9 provide no additional information because the boundary-layer flow on the bottom of the fuselage is obscured by the pylon and the flow on the top is affected by the canopy. (See ref. 2.) Changing the X-15 nozzle from nozzle A to nozzle B had only a slight effect on the surface pressures as shown by figure 11. Data which have not been presented indicate that increasing the ramjet pressure ratio from 10 to over 20 had only a slight effect on the surface pressures.

Ramjet Exhaust Impingement Effects on the Nozzle Extension

The results of the investigation of the ramjet exhaust impingement on the nozzle extension of the X-15 model (nozzle B, with and without manifold ring) are presented in figures 12 to 17. In figures 12 and 15 (for nozzles B1 and B2, respectively), the

static-pressure data are presented in two types of plots. The plots on the left-hand side of these figures present the static-pressure ratios at each measuring orifice as a function of the pressure ratios of the ramjet engine simulator. Longitudinal static-pressure-ratio distributions are shown in the plots on the right-hand side of these figures. The pressure subscript numbers in figures 12 and 15 correspond to the orifice numbers indicated in figure 3 and in the sketches at the top of figures 12(a) and 15(a). The value of $p_{j,ram}/p_\infty$ for exhaust impingement on the individual orifices and the longitudinal location of impingement on the X-15 nozzle were obtained from figure 14 (nozzle B1, no ring) and are indicated by arrows in figures 12, 15, and 17. It should be noted that the vertical scales are not the same for all the curves presented in figures 12 and 15. These scales were arbitrarily selected for clarity in presenting the data.

External pressures on the nozzle extension.- The static-pressure ratio along the external surface of nozzle B1 are presented in figure 12(a) for the model at an angle of attack of 0^o. Both sets of curves in this figure show that the impingement point of the ramjet exhaust on the nozzle extension moves forward along the extension as the ramjet pressure ratio increases. However, pressures at orifices 4 and 5 were essentially unaffected by changes in the ramjet pressure ratio.

Reference 8 indicated that nozzle exhaust plumes impinging upon a parallel flat plate resulted in plate surface pressures peaking near the impingement zones. For the longitudinal pressure-ratio distributions of figure 12(a), curve fairings which would show peak pressures at the impingement zones (indicated by arrows) would require extensive interpolations in the fairings, particularly for $p_{j,ram}/p_\infty = 20$ and 60. Therefore, for these two pressure ratios, the fairing of the curves has been omitted in the areas of impingement.

Impingement effects upon the nozzle external pressures for the X-15 model positioned at an angle of attack of 3^o are presented in figure 12(b). The general trend is similar to that observed for the model positioned at an angle of attack of 0^o but somewhat delayed; that is, for any given longitudinal position, peak pressures occur at higher values of $p_{j,ram}/p_\infty$. The delay is evident by comparing the individual orifice pressure ratios. For example, the pressure at orifice 6 has not reached a peak value over the test ramjet pressure ratio for an angle of attack of 3^o; whereas, a peak value was obtained for an angle of attack of 0^o (fig. 12(a)).

Schlieren photographs, which correspond to the pressure data results of figure 12, are presented in figures 13(a) and 13(b) for the model positioned at angles of attack of 0^o and 3^o, respectively. All pressure ratios may not be represented by schlieren photographs because of the poor quality of some of the photographs. The rows of photographs represent the different free-stream conditions as denoted at the right of each row. The photographs indicate an area of slight impingement near the exit of the nozzle extension

even at the lowest pressure ratios. Plume initial turning angles appear to be greater in the photographs than indicated by the calculations presented in figure 7. This difference may be due to the fact that the free-stream flow was assumed to be undisturbed for the calculations of figure 7. Also, the plumes appear to have greater expansion on the top side (adjacent of X-15 fuselage) than on the bottom side – probably because of a wake from the ramjet-pylon combination.

Enlargements of the schlieren photographs shown in figure 13 were used to obtain exhaust-impingement locations on nozzle B1; the locations for $\alpha = 0^{\circ}$ and 3° are presented in figure 14. The various free-stream conditions ($p_{t,\infty}$ = 5, 10, 17.5 atmospheres) appeared to have little effect upon the impingement locations; therefore, the two curves are representative variations of the locations for all test conditions. The curves indicate that the ramjet plume initially impinged upon the X-15 nozzle extensions at values of $p_{j,ram}/p_{\infty}$ of 8 and 12 for the model positioned at angles of attack of 0° and 3°, respectively.

External pressures on the nozzle extension with an attached manifold ring.- The results from tests of nozzle B2 are presented in figure 15. The pressure distributions along the nozzle (right-hand plots) have the center of the ring location denoted on each abscissa by a tick.

Comparisons of the pressure distributions of figure 15 with those of figure 12 show that the ring does have an effect upon the external pressures of the nozzle extension. This result was expected since the ring is relatively large and a significant shock system would be created by the ring. The low pressures noted for orifice 7 result from the close proximity of this orifice to the downstream side of the ring. From figure 14 and enlarged prints of the schlieren photographs (fig. 13), the plume boundary was found to contact the ring initially at $p_{j,ram}/p_{\infty}$ of 13 and impinge at the nozzle-ring tangent point at $p_{j,ram}/p_{\infty}$ of approximately 22; these pressure-ratio values became approximately 20 and 40, respectively, for the tests with the model at an angle of attack of 3° (fig. 15(b)). Since ramjet exhaust plume and manifold ring disturbances interacted strongly in this pressure-ratio range resulting in a complex shock system and flow disturbances, the locations of peak pressures at impingement zones, as indicated in reference 8, become undeterminable. The schlieren photographs for nozzle B2 at angles of attack of 0° and 3° are presented in figures 16(a) and 16(b), respectively.

Another demonstration of the effect of the ring is illustrated by the comparisons, presented in figure 17, of the pressure distributions along nozzles B1 and B2 for free-stream total pressures of 10 atmospheres. Approximations were made to determine the change in upward force on extended nozzles B1 and B2, caused by changing the ramjet nozzle from the nonoperating condition to a pressure ratio of 10. These approximations showed that ramjet operation would cause increases in the upward force on the two

full-scale X-15 nozzles of approximately 1210 and 760 newtons for nozzles B1 and B2, respectively, for an angle of attack of 0°. For the model at an angle of attack of 3°, results indicated that the changes in forces would be about 1330 and 1180 newtons for nozzles B1 and B2, respectively.

The foregoing discussion showed that even at low ramjet pressure ratios the ramjet plume will impinge upon the X-15 nozzle extension. However, it should be noted that the test ramjet nozzle had a flow angle θ_n of 15° and the incorporation of smaller flow angles at the ramjet nozzle exit would result in smaller initial plume turning angles. The smaller initial turning angles may, in turn, prevent the plume from impinging upon the adjacent X-15 nozzle extension at the very low ramjet pressure ratios.

CONCLUDING REMARKS

An investigation has been conducted to determine the effects of underexpanded ramjet exhaust gases on the external surface pressures on adjacent X-15 nozzle extension and to determine the effect of the disturbance from the simulated ramjet on the X-15 afterbody pressures.

Results showed that the ramjet nozzle exhaust plume initially impinged upon the nonblowing X-15 nozzle extension at low values of ramjet pressure ratio (ratio of ramjet nozzle-exit pressure to ambient static pressure), 8 and 12 for angles of attack of 0° and 3°, respectively.

The presence of the ramjet and its support pylon affected the X-15 afterbody surface pressures. Without the ramjet attached, all the surface pressures increased with increased X-15 nozzle-exit pressure, but when the ramjet was attached, the pressures tended to remain constant. The pressure-measuring station nearest the base of the fuselage did, however, show a pressure rise as the external expansions of the X-15 nozzle exhaust gases increased. In this investigation, the inlet of the ramjet was not simulated and therefore the proper flow field between the X-15 and ramjet was not produced. This, together with the fact that the model boundary layer was predominantly laminar, prevents direct application of the measured afterbody surface pressures to flight conditions.

A collecting manifold ring positioned near the exit of the X-15 nozzle extension resulted in a system of shock and expansion waves about the ring. The shock and expansion waves resulted in higher pressure readings immediately upstream of the ring and lower pressures immediately downstream; this effect was especially true for the large ramjet pressure ratios. Changes in upward forces on a full-scale nozzle extension, with and without the manifold ring, were approximated (differences between forces for no ramjet exhaust and those for a ramjet exit-to-ambient static-pressure ratio of 10). Forces

on the extension without the ring were greater than those with the ring. The possible effect of these forces on the structural integrity of the extension was beyond the scope of this investigation.

Langley Research Center,
National Aeronautics and Space Administration,
Langley Station, Hampton, Va., March 13, 1967,
126-15-03-16-23.

REFERENCES

1. Dugger, Gordon L.: A Future for Hypersonic Ramjets. Astronautics, vol. 4, no. 4, Apr. 1959, pp. 38-39, 114-117.

2. Fetterman, David E., Jr.: Effects of Simulated Rocket-Jet Exhaust on Stability and Control of a Research-Type Airplane Configuration at a Mach Number of 6.86. NASA TM X-127, 1959.

3. McLellan, Charles H.; Williams, Thomas W.; and Beckwith, Ivan E.: Investigation of the Flow Through a Single-Stage Two-Dimensional Nozzle in the Langley 11-Inch Hypersonic Tunnel. NACA TN 2223, 1950.

4. Anon.: U.S. Standard Atmosphere, 1962. NASA, U.S. Air Force, and U.S. Weather Bur., Dec. 1962.

5. Wang, C. J.; Peterson, J. B.; and Anderson, R.: Gas Flow Tables. GM-TR-154, Space Tech. Labs., Inc., Mar. 14, 1957. (Available from ASTIA as AD No. 221012.)

6. Love, Eugene S.; Grigsby, Carl E.; Lee, Louise P.; and Woodling, Mildred J.: Experimental and Theoretical Studies of Axisymmetric Free Jets. NASA TR R-6, 1959. (Supersedes NACA RM L54L31 by Love and Grigsby; RM L55J14 by Love; RM L56G18 by Love, Woodling, and Lee; and TN 4195 by Love and Lee.)

7. Dennard, John S.; and Spencer, Patricia B.: Ideal-Gas Tables for Oblique-Shock Flow Parameters in Air at Mach Numbers From 1.05 to 12.0. NASA TN D-2221, 1964.

8. Vick, Allen R.; and Andrews, Earl H., Jr.: An Experimental Investigation of Highly Underexpanded Free Jets Impinging Upon a Parallel Flat Surface. NASA TN D-2326, 1964.

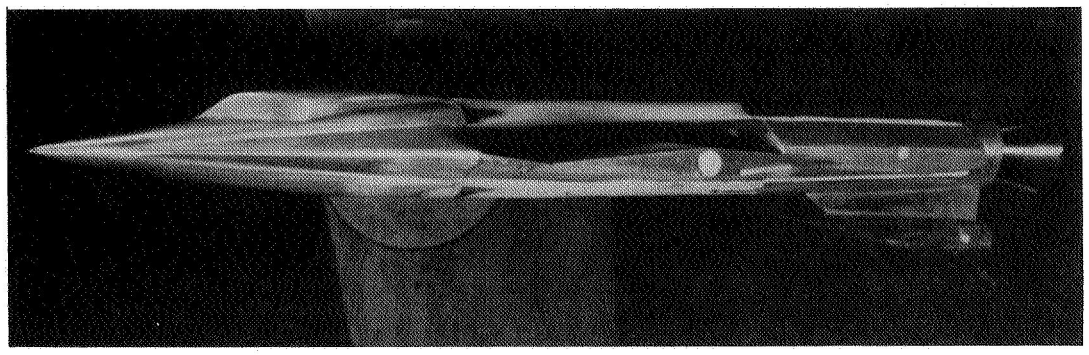

(a) Three-quarter front view.

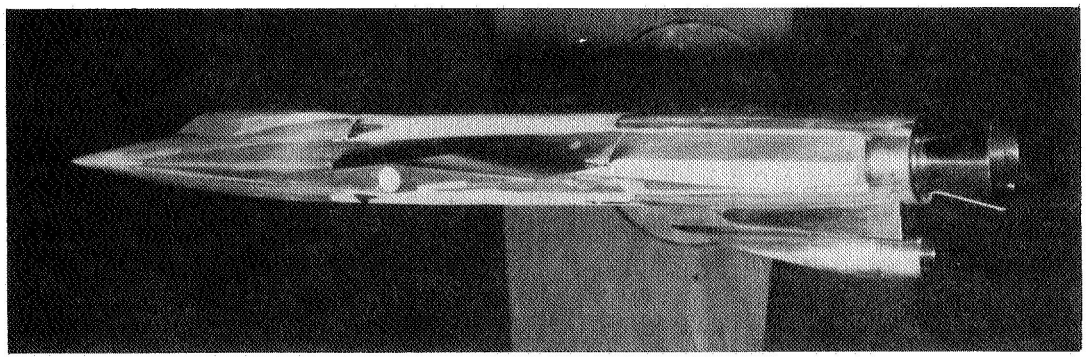

(b) Three-quarter rear view.

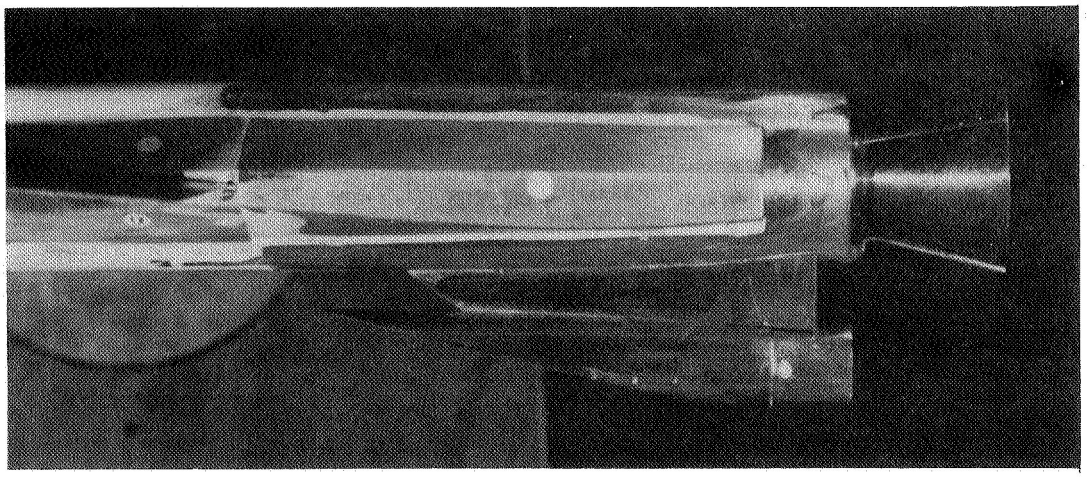

(c) Base-area side view.

L-67-1056

Figure 1.- Photographs of the 0.02-scale X-15 model with extended nozzle $(M_j = 4.1)$ and with attached ramjet engine simulator.

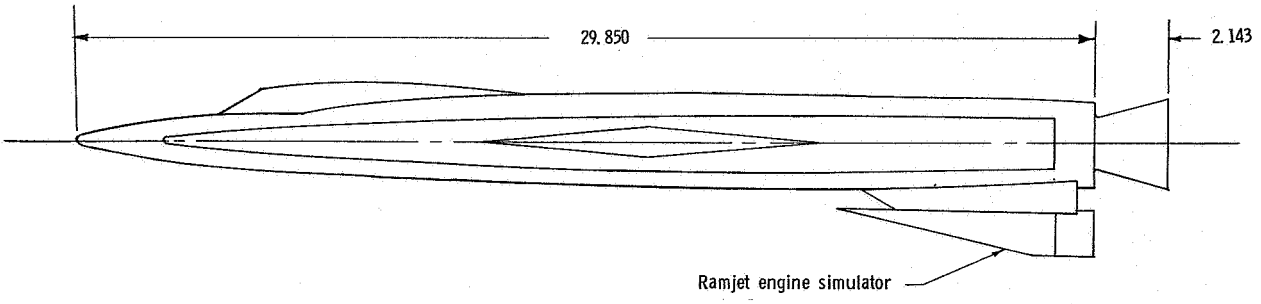

Side view

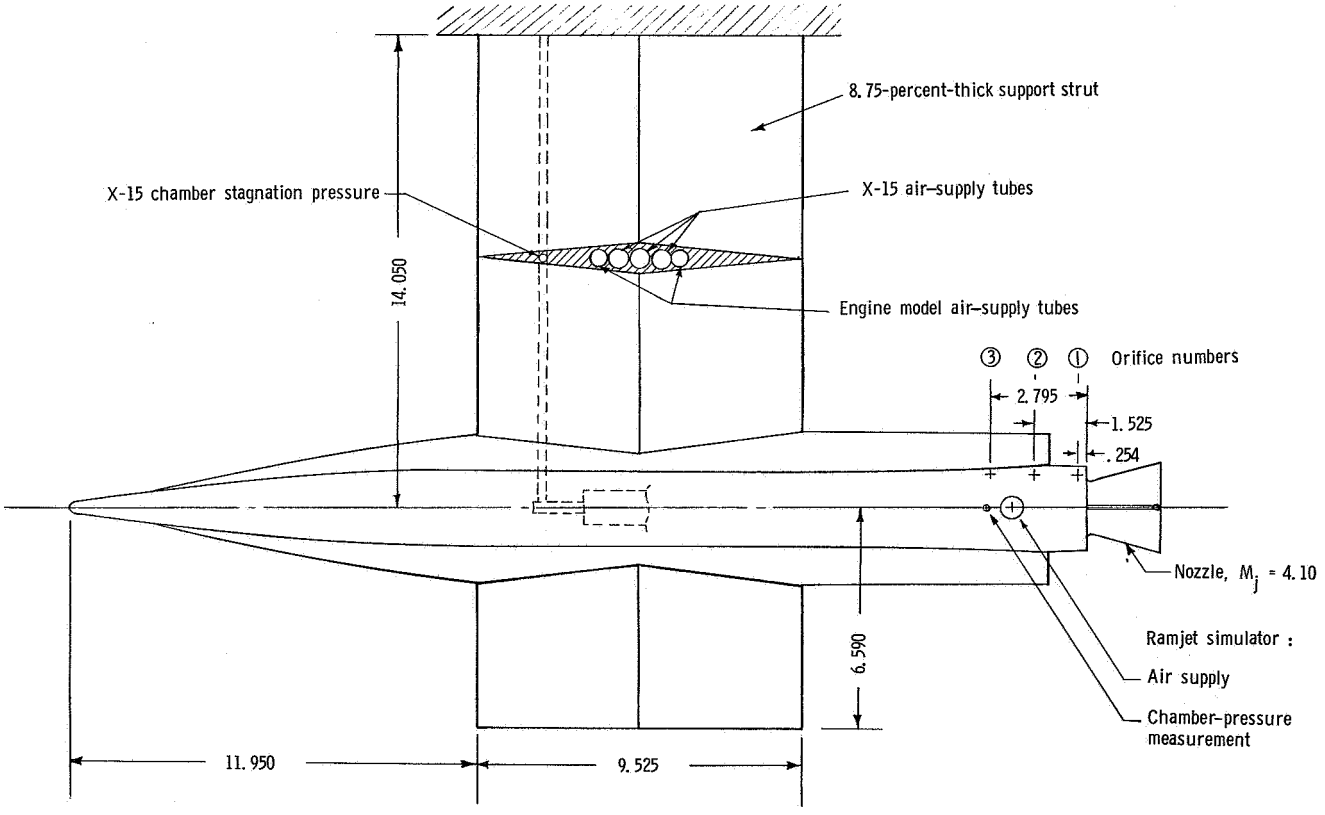

Bottom view (ramjet simulator removed)

Figure 2.- Details of the X-15 model with the extended nozzle and with the attached ramjet engine simulator. All dimensions in centimeters.

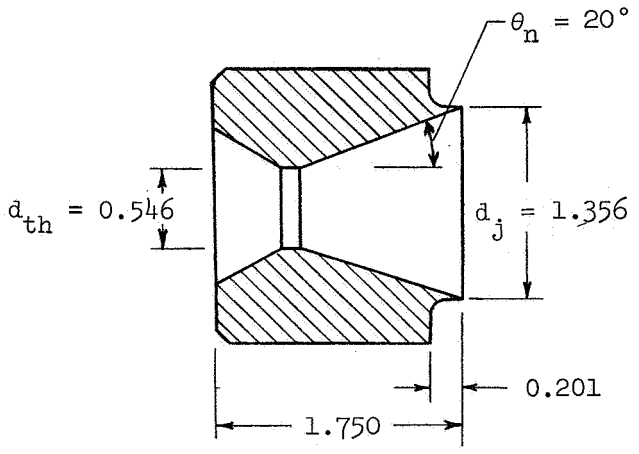

(a) Nozzle A. M_j = 3.4.

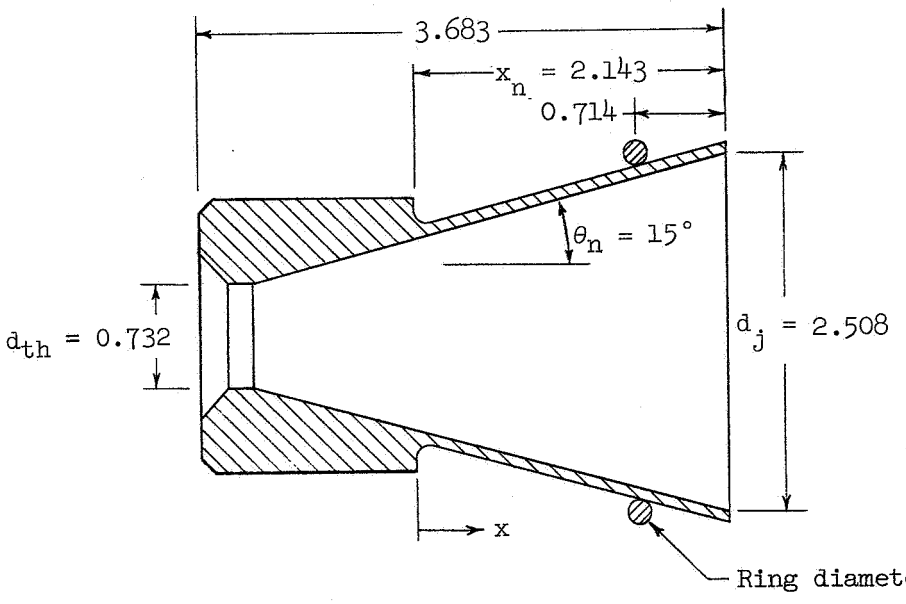

External static pressure orifice locations (underside of nozzle)

No.	x, cm
4	0.493
5	.874
6	1.255
7	1.636
8	2.018

Orifice diameter = 0.01

(b) Nozzle B (without ring designated B1, with ring designated B2). M_j = 4.1.

Figure 3.- Details of the X-15 nozzles. All dimensions in centimeters.

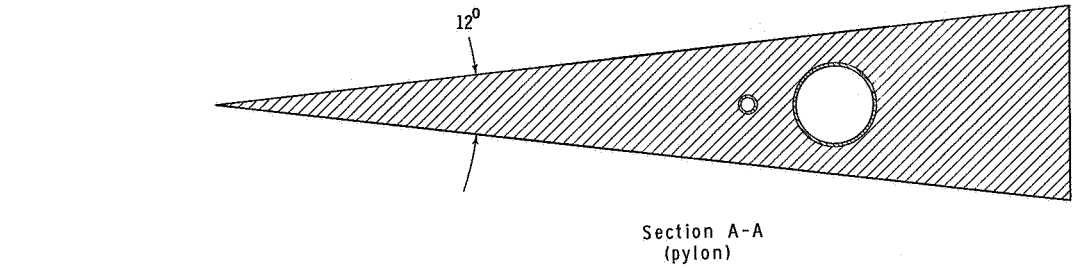

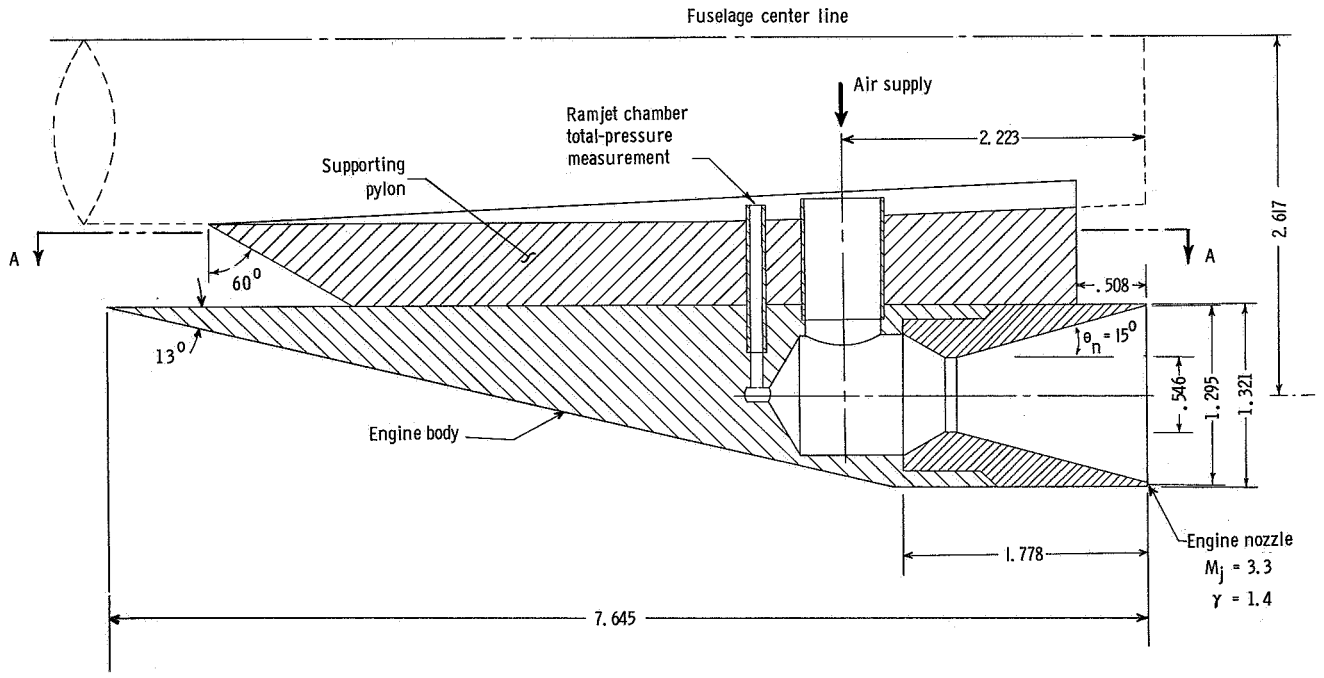

Figure 4.- Details of the ramjet engine simulator and support pylon. All dimensions in centimeters.

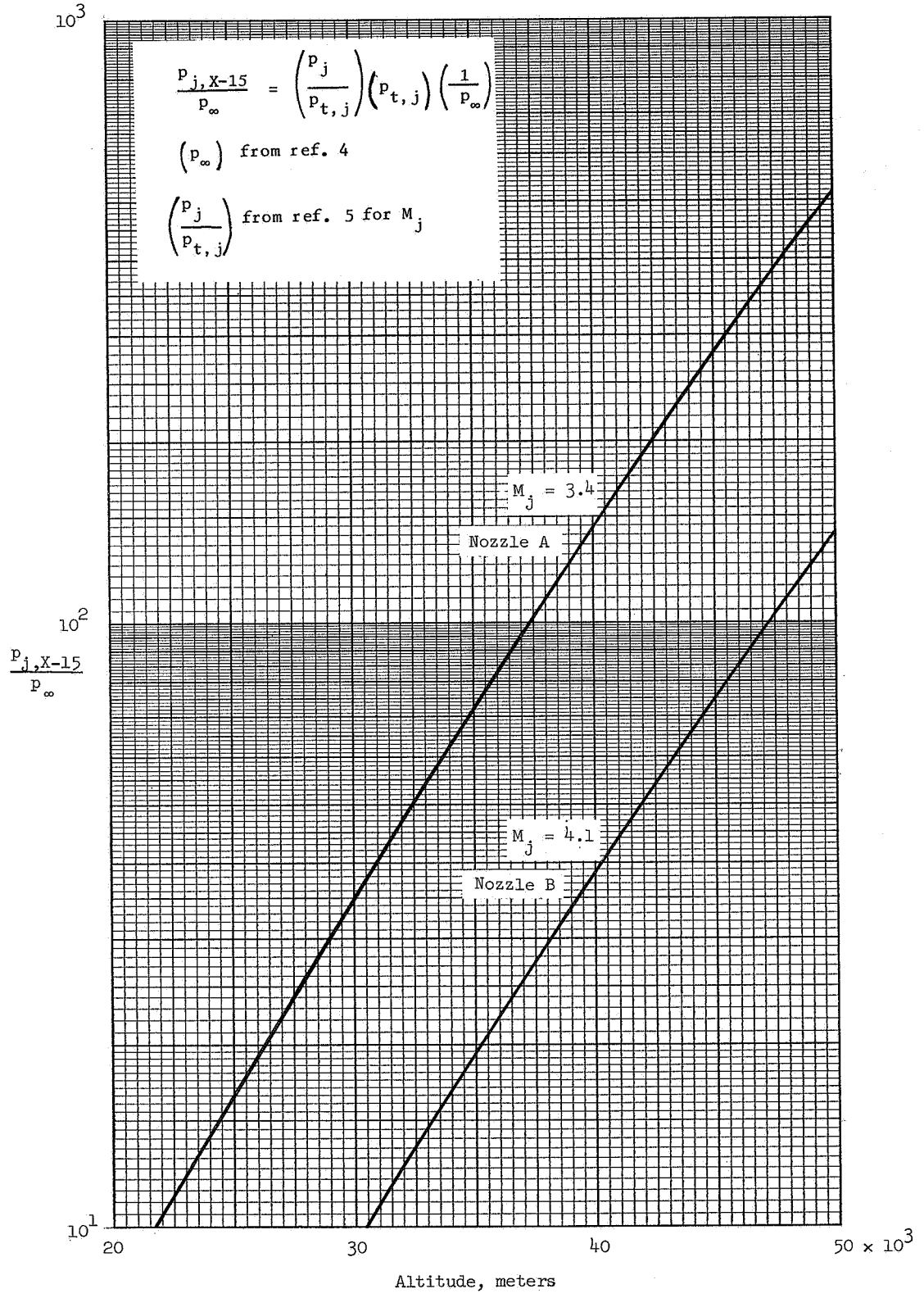

Figure 5.- Effect of altitude on X-15 exit-to-ambient static-pressure ratio. $p_{t,X-15} = 40.8$ atmospheres; $\gamma = 1.2$.

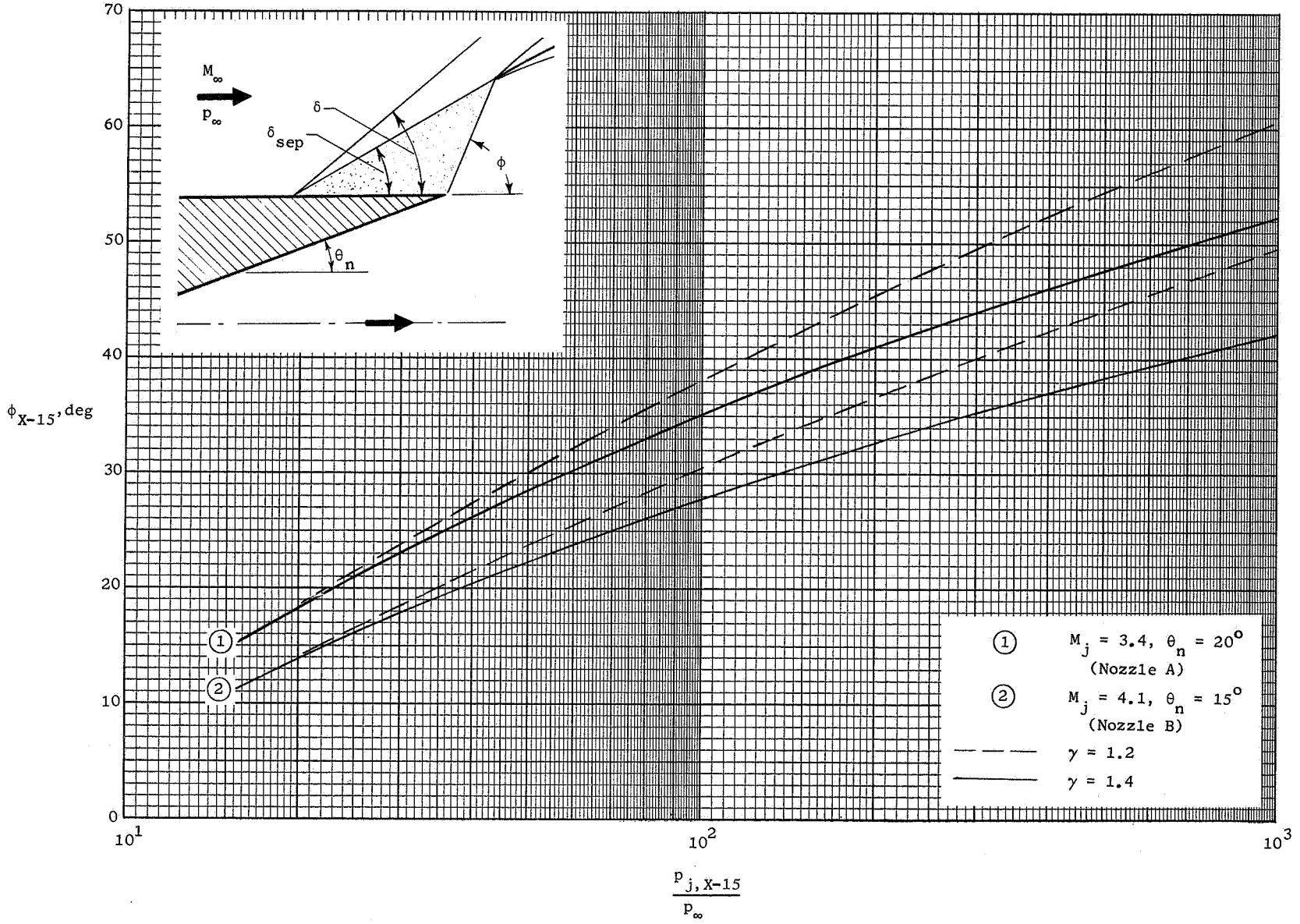

Figure 6.- Initial turning angle of X-15 nozzle exhaust gases. $M_\infty = 6.86$; $\delta_{sep} = 30^o$; $\delta = 40^o$.

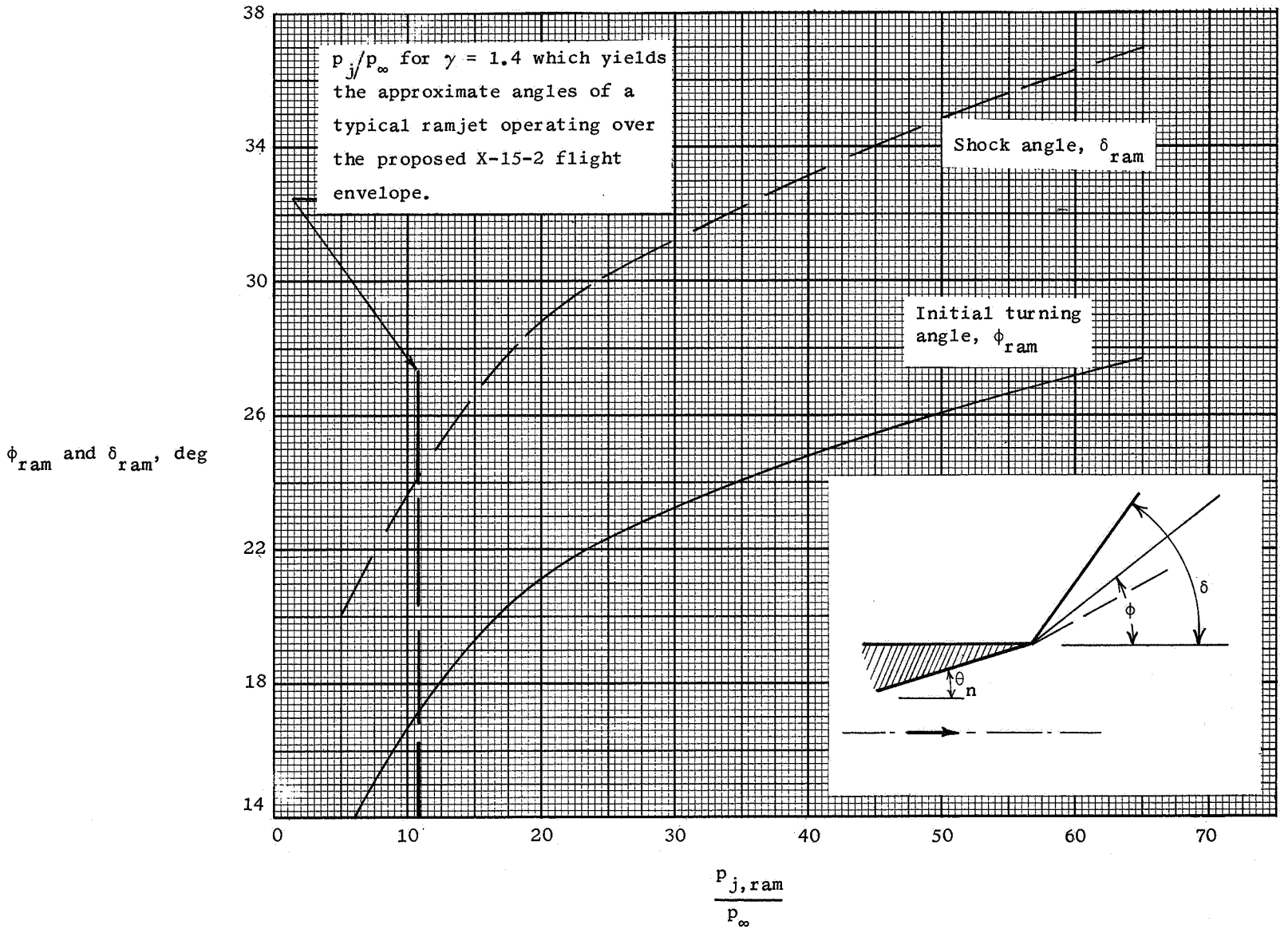

Figure 7.- Initial plume expansion and shock angles of the ramjet engine simulator. M_j = 3.3; γ = 1.4; $\theta_n = 15^0$. (Assumed undisturbed, attached, two-dimensional flow at nozzle lip for M_∞ = 6.86.)

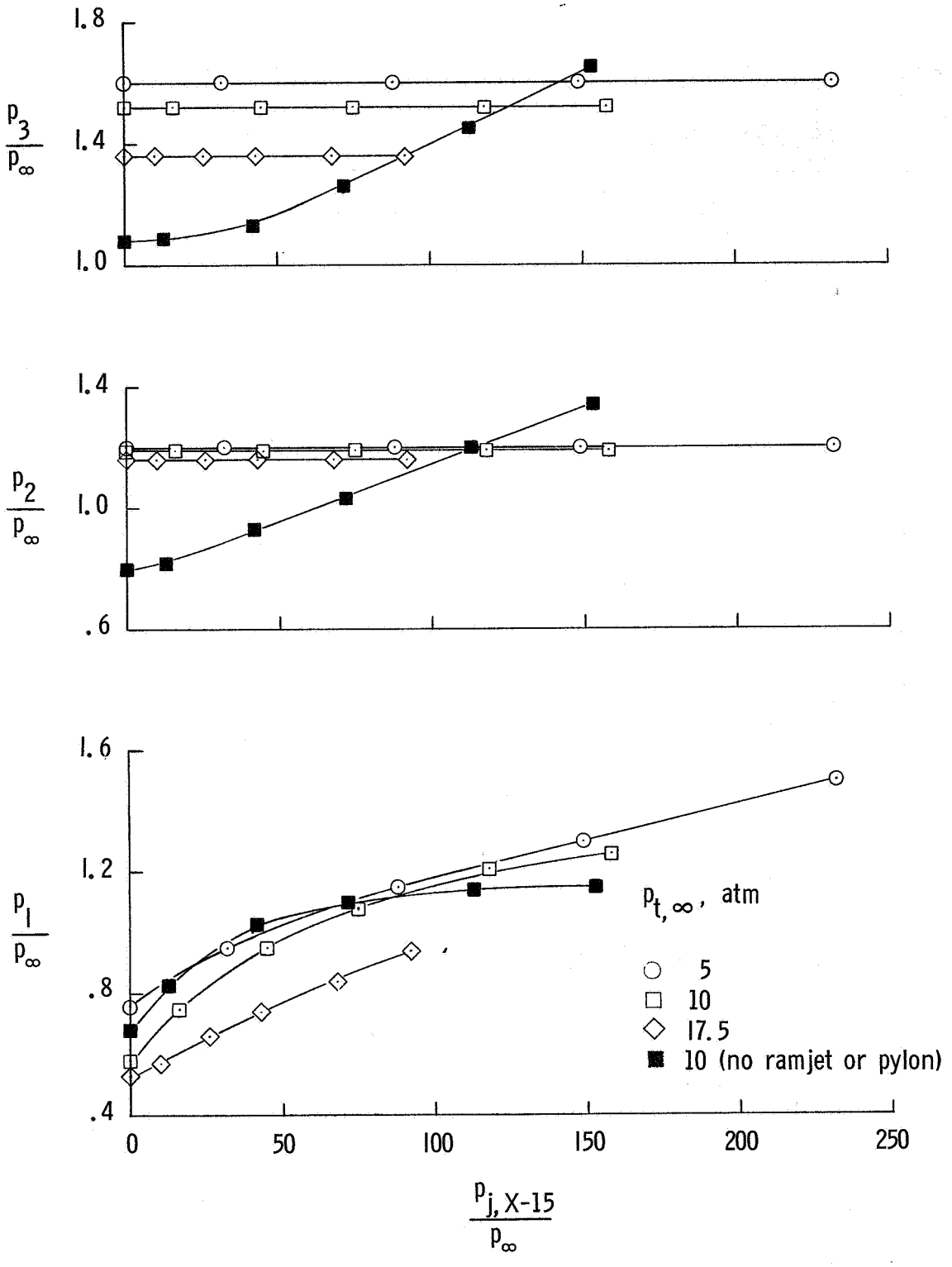

Figure 8.- Effect of exhaust gas expansions upon the model fuselage surface pressures. Nozzle B; $\alpha = 0^o$; $p_{j,ram}/p_\infty \approx 10$.

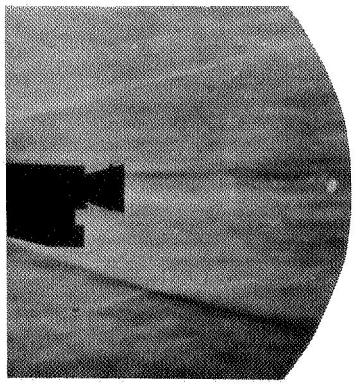

(a) Jets off.

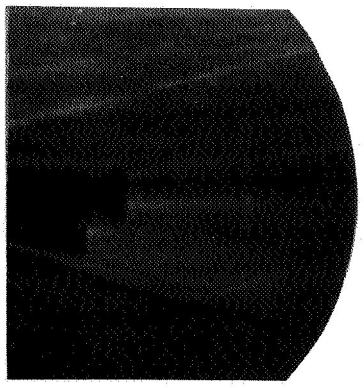

(b) $p_{j,ram}/p_{\infty} = 10.$

(c) $p_{j,X-15}/p_{\infty} = 32.$

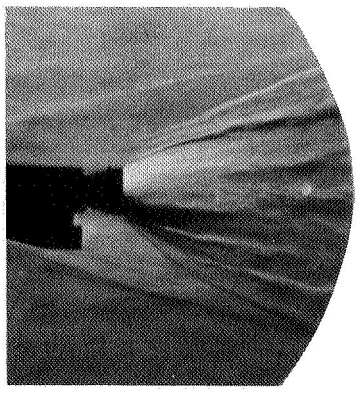

(d) $p_{j,X-15}/p_{\infty} = 88.$

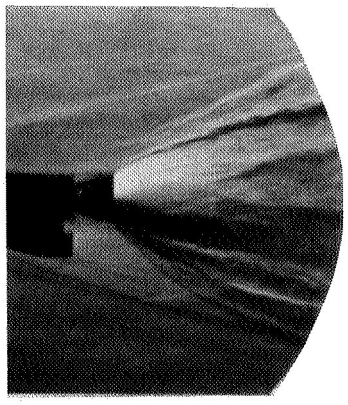

(e) $p_{j,X-15}/p_{\infty} = 148.$

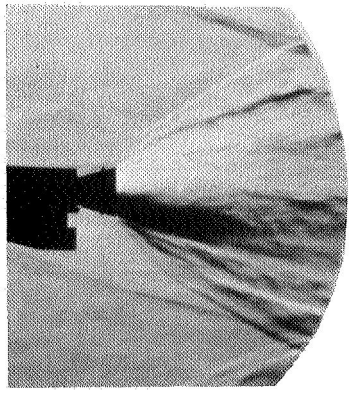

(f) $p_{j,X-15}/p_{\infty} = 233.$

L-67-1057

Figure 9.- Schlieren photographs showing flow fields in relation to the various amounts of nozzle exhaust gas expansion. Nozzle B2; $\alpha = 0^{0}$; $p_{t,\infty} = 5$ atmospheres. (Pressure ratios correspond to those of fig. 8.)

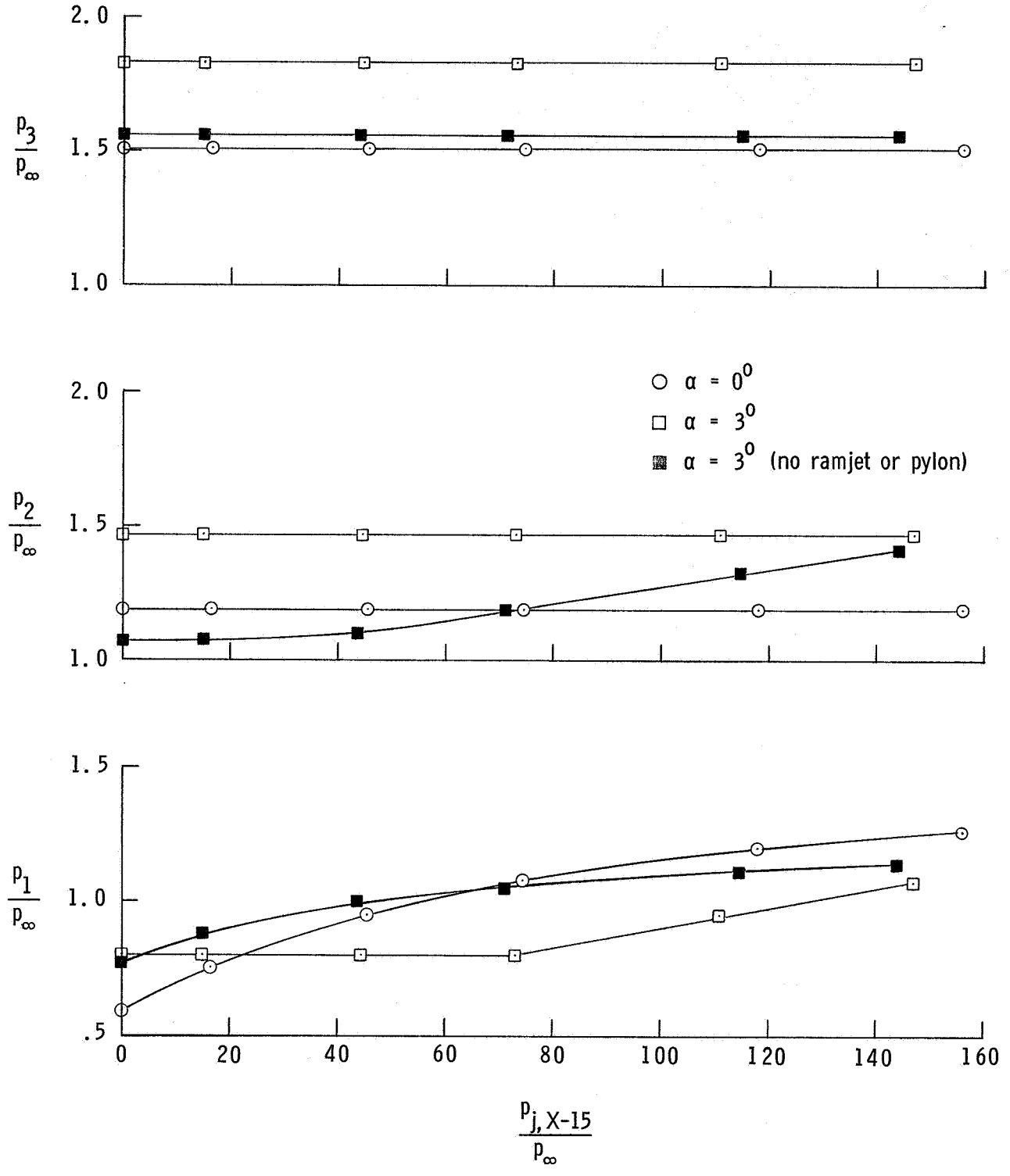

Figure 10.- Comparison of the exhaust gas expansion effect upon the model fuselage surface pressures for angles of attack of 0^0 and 3^0. Nozzle B; $p_{j,ram}/p_\infty \approx 10$; $p_{t,\infty} = 10$ atmospheres.

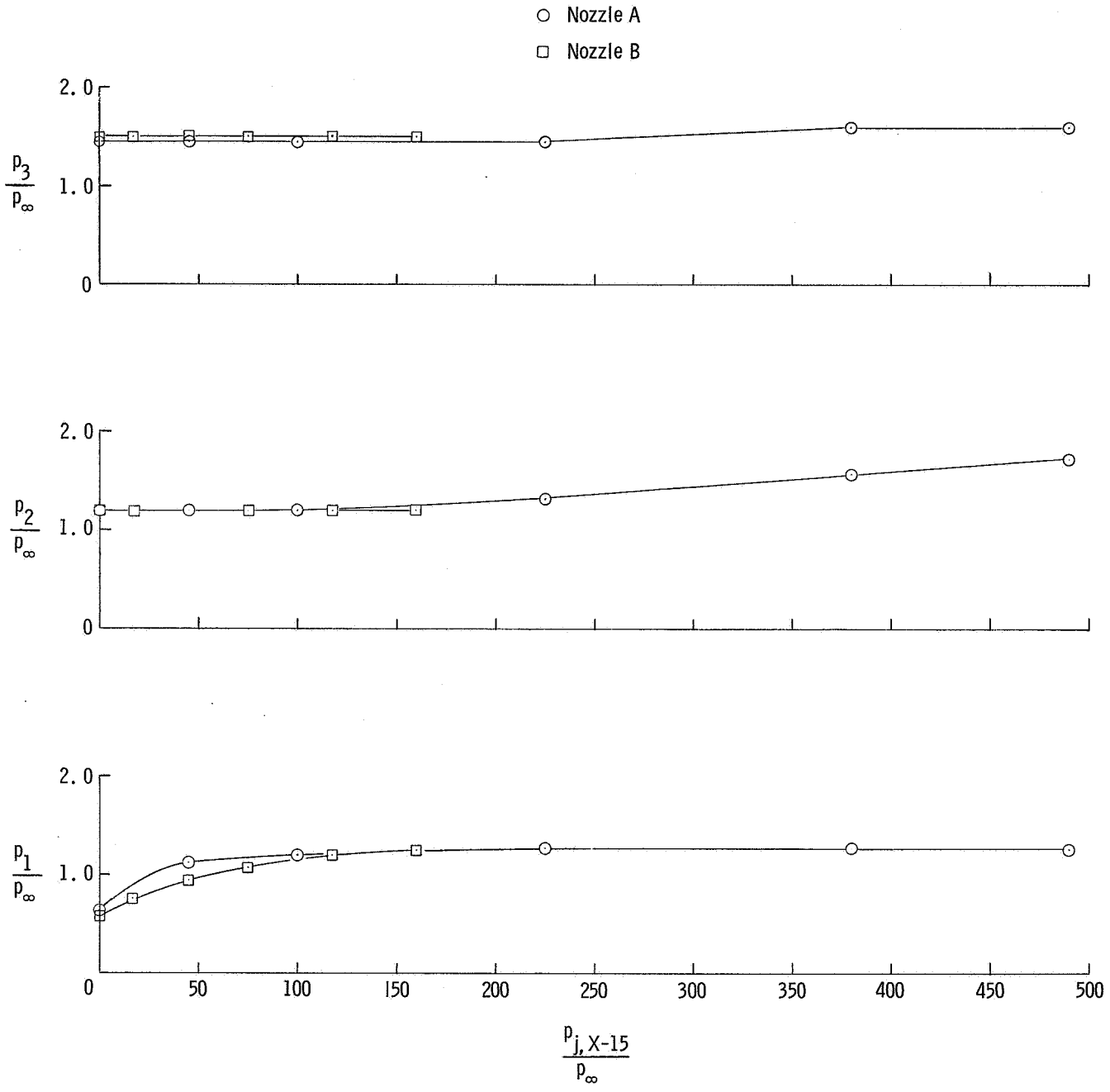

Figure 11.- Comparison of the exhaust gas expansion effect upon the model fuselage surface pressures for the two X-15 nozzles. $p_{j,ram}/p_\infty \approx 10$; $p_{t,\infty} = 10$ atmospheres; $\alpha = 0^o$.

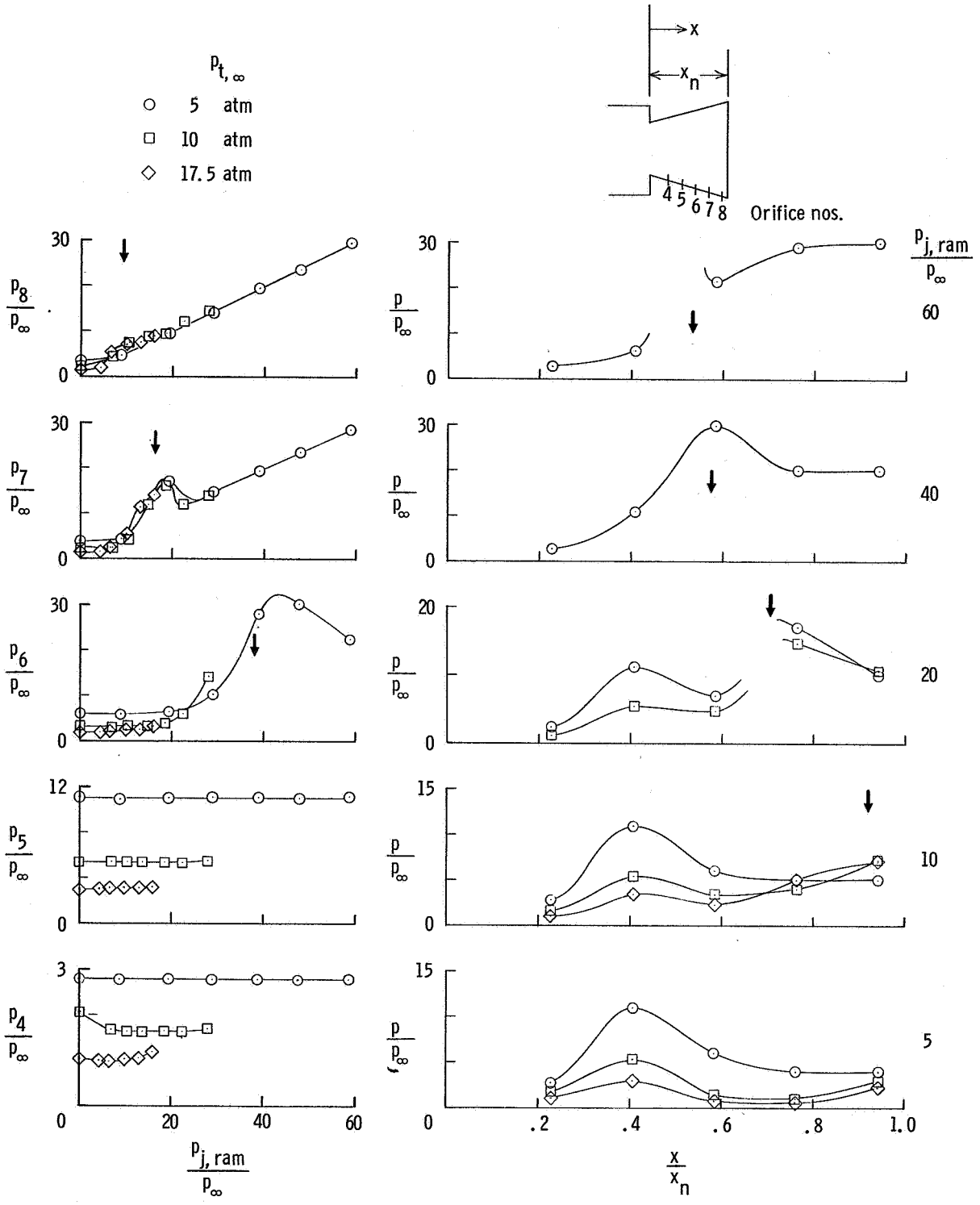

(a) $\alpha = 0^o$.

Figure 12.- Effect of ramjet exhaust gas expansion upon the external pressures of nozzle B1. $p_{t,X-15} = 0$. Arrows denote impingement zone.

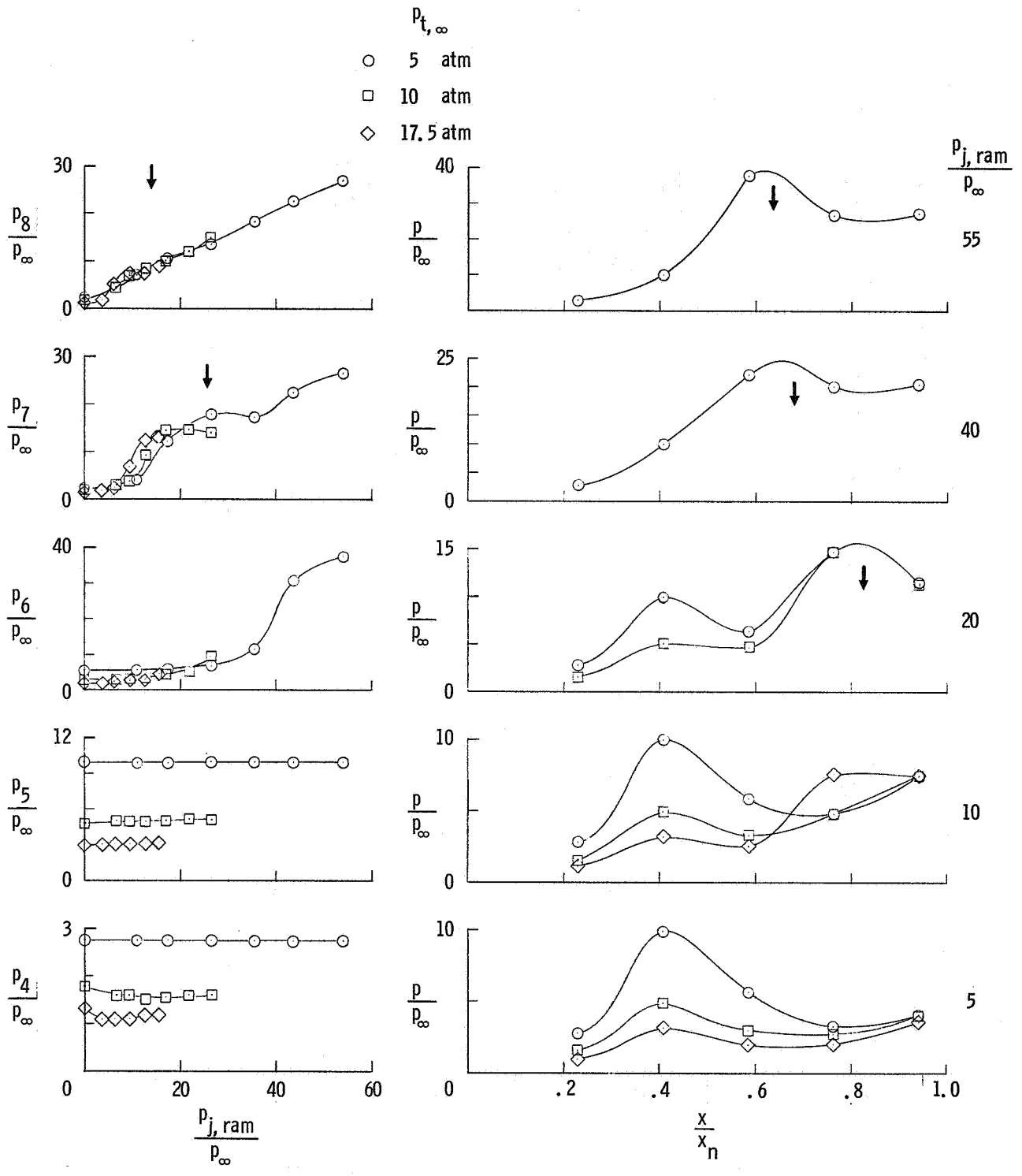

(b) $\alpha = 3^o$.

Figure 12.- Concluded.

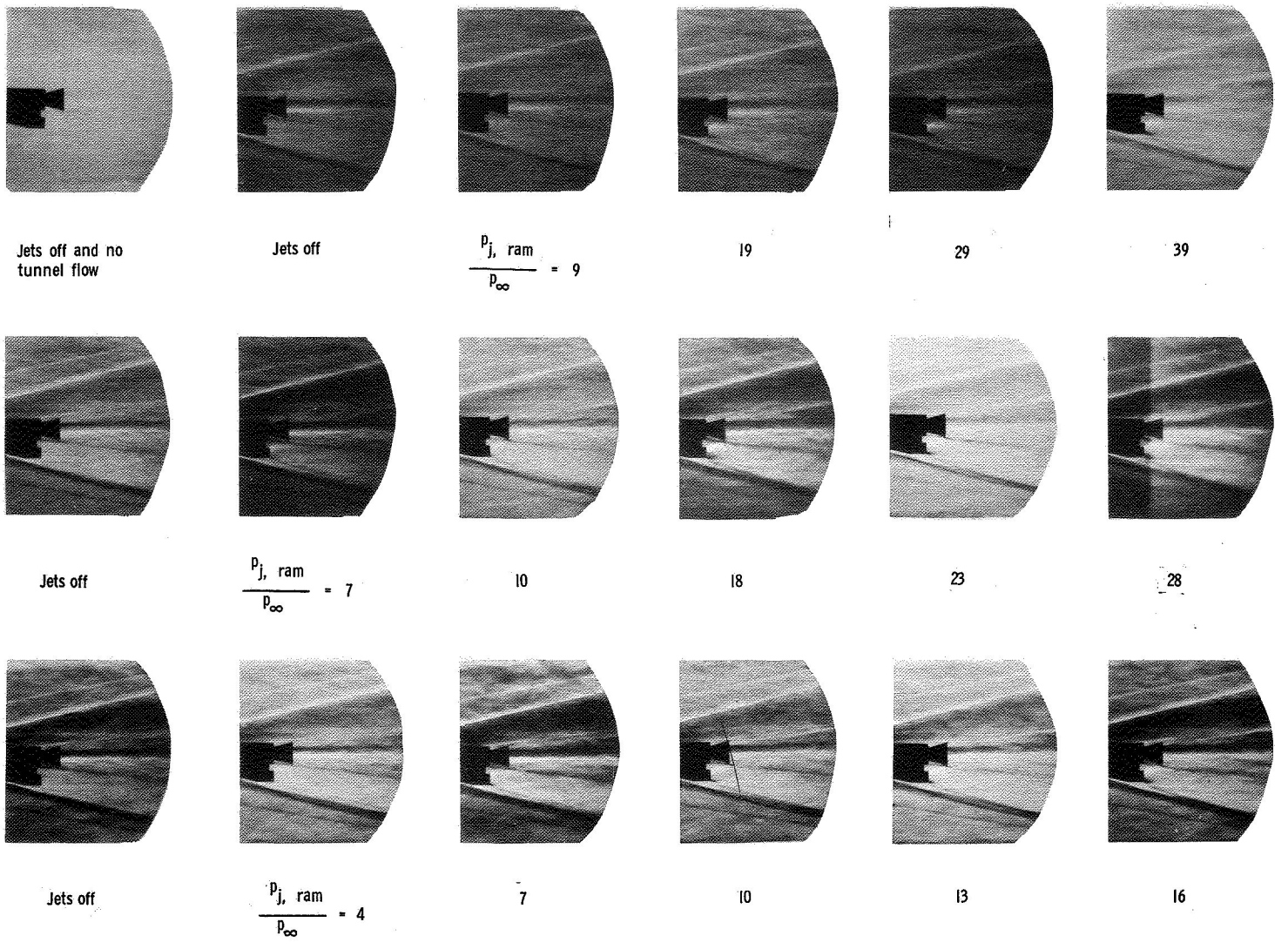

(a) $\alpha = 0^0$.

L-67-1058

Figure 13.- Schlieren photographs showing ramjet engine simulator exhaust impinging on nozzle B1. $p_{t,X-15} = 0$.

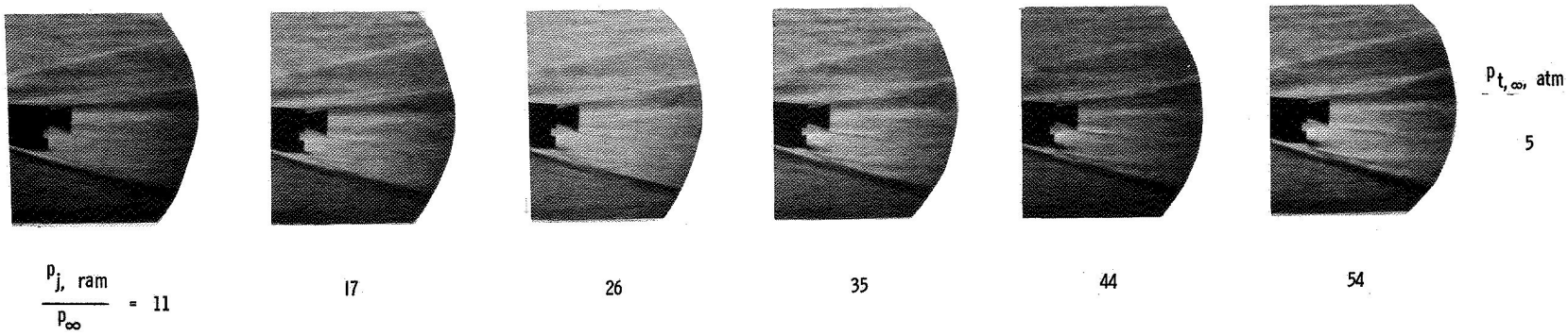

(b) $\alpha = 3^{o}$.

Figure 13.- Concluded.

L-67-1059

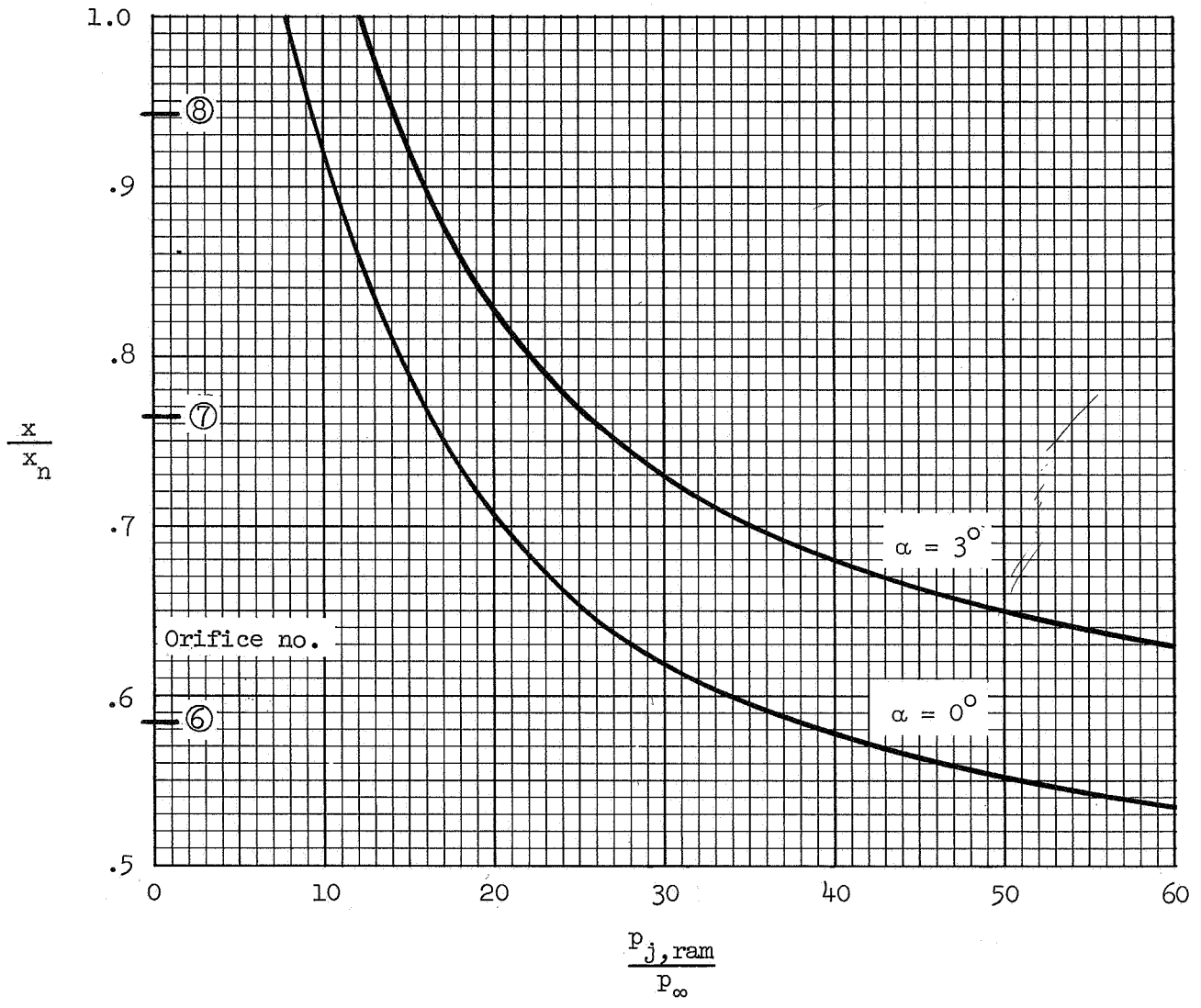

Figure 14.- Variation of the location of the ramjet engine exhaust impingement on nozzle B1 with the ramjet exit-to-ambient pressure ratio.

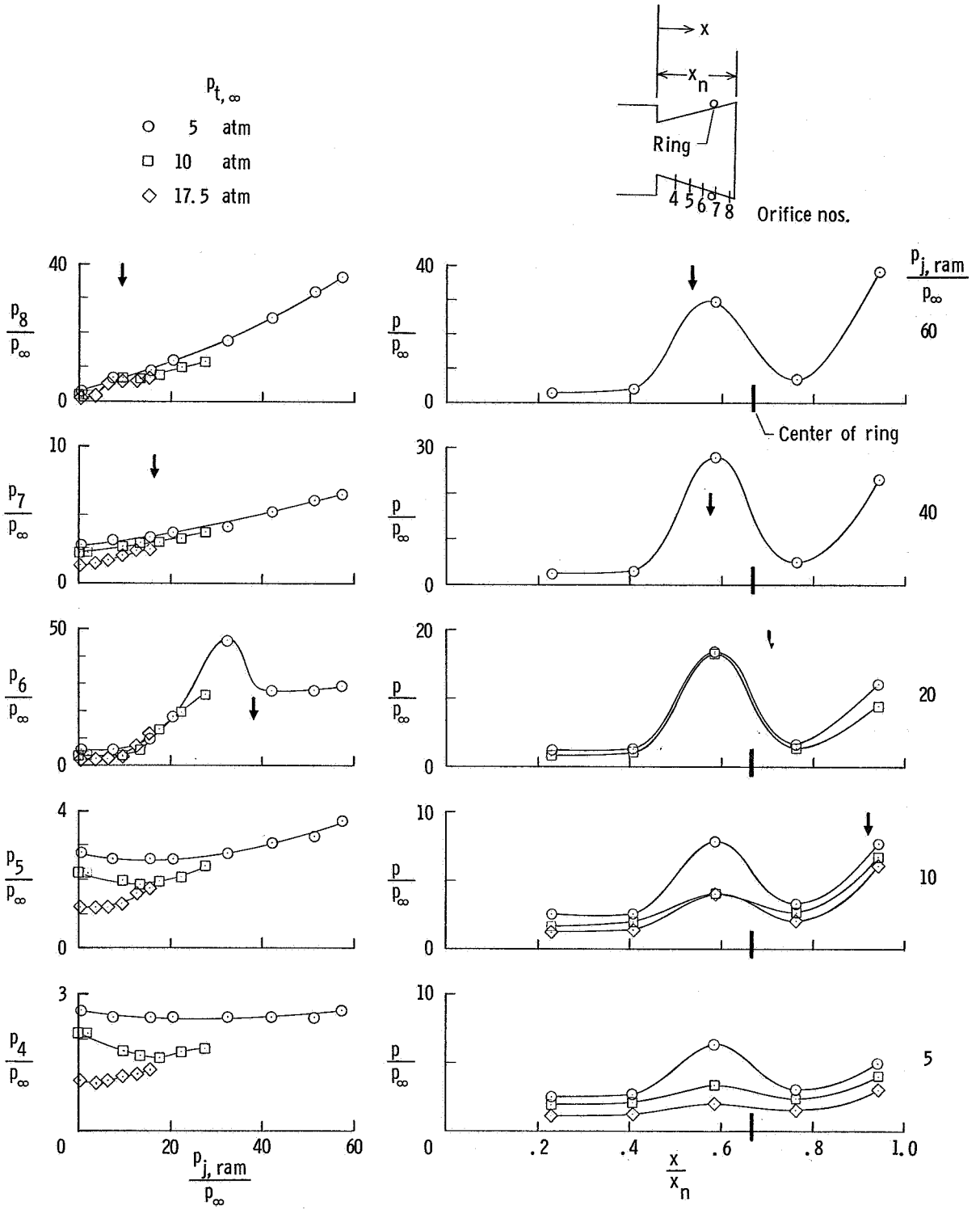

(a) $\alpha = 0^o$.

Figure 15.- Effect of ramjet exhaust gas expansion upon the external pressures of nozzle B2. $p_{t,X-15} = 0$. Arrows denote impingement zone; long tick marks denote center of ring.

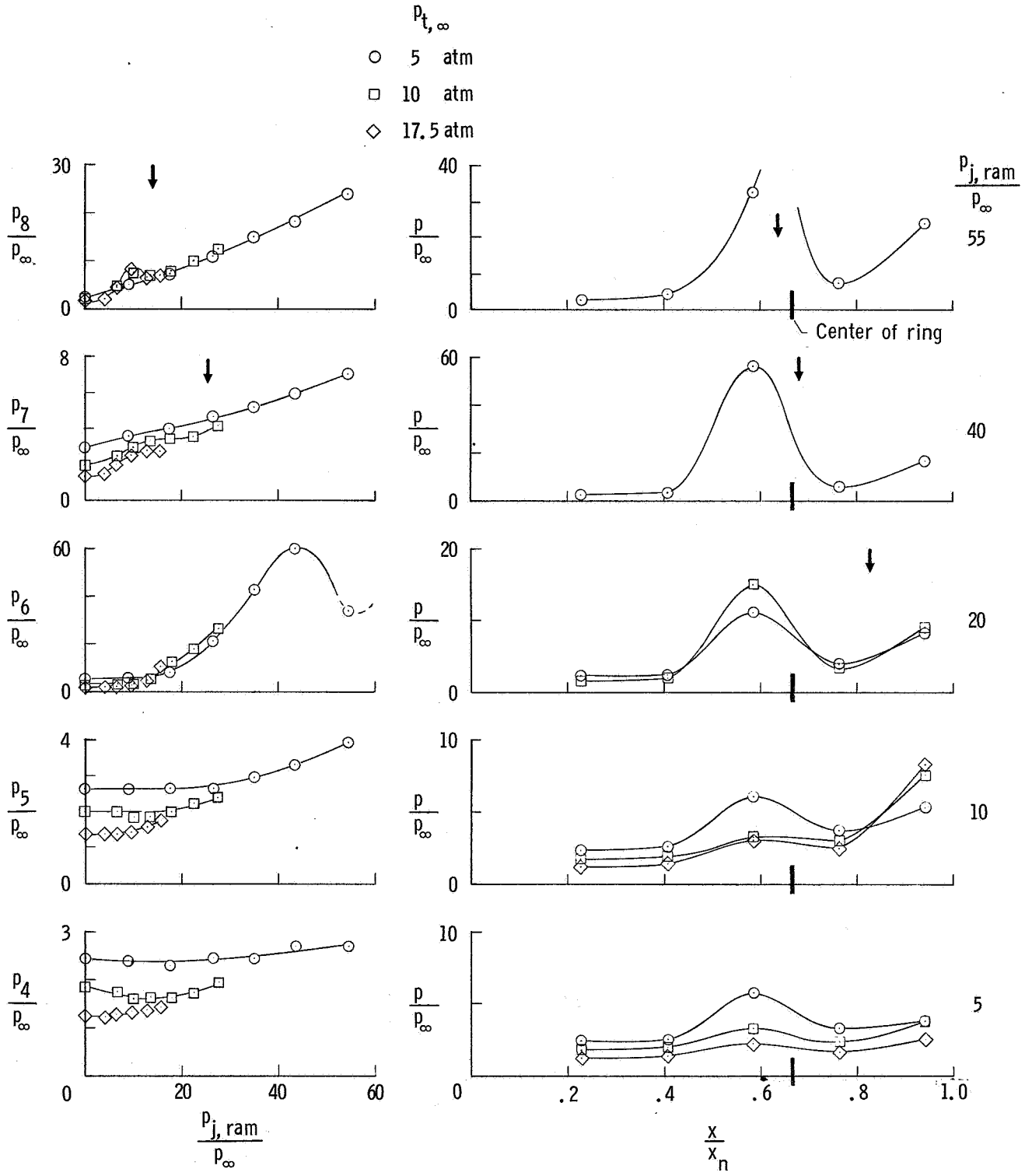

(b) $\alpha = 3^0$.

Figure 15.- Concluded.

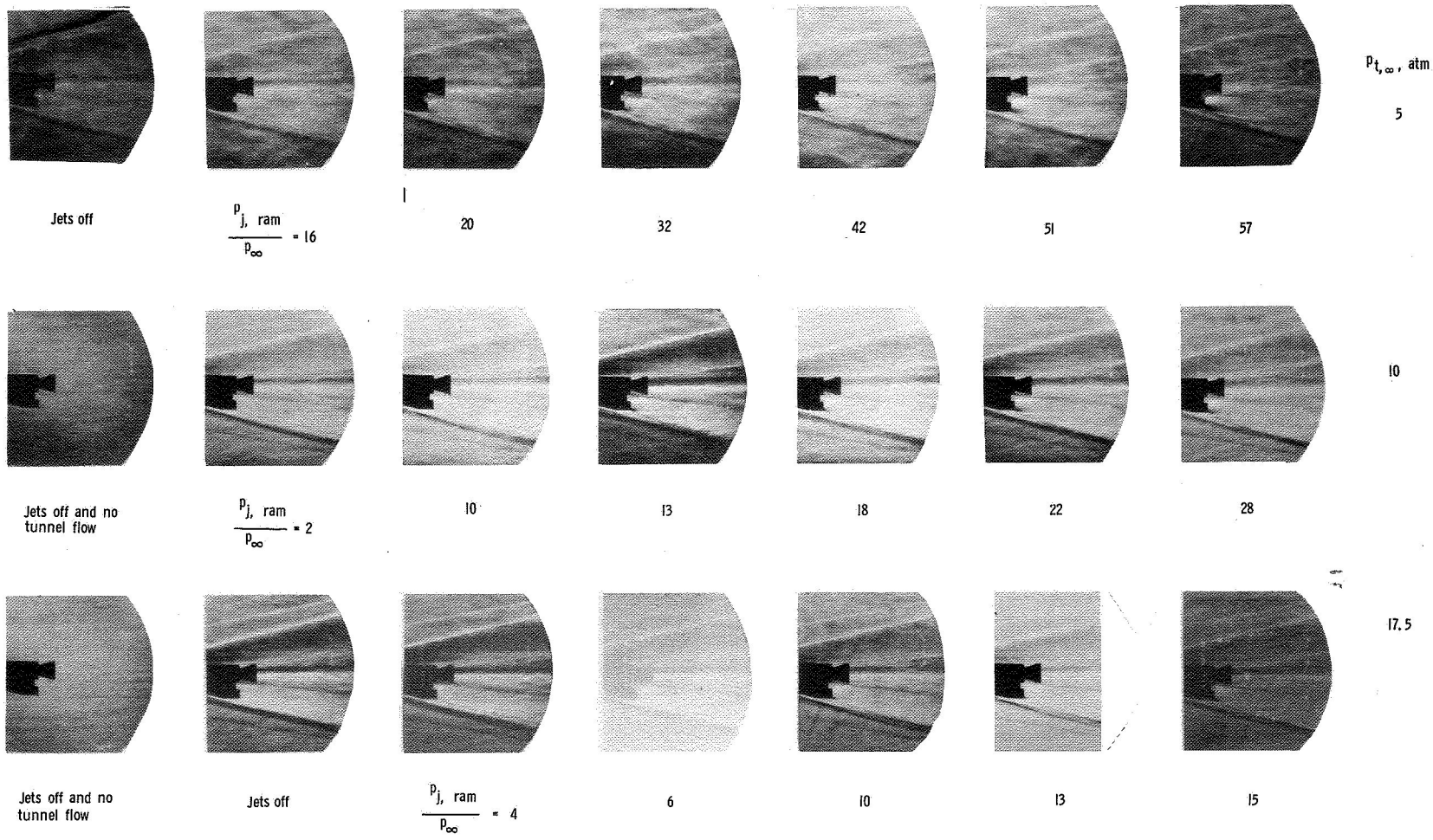

(a) $\alpha = 0^0$.

L-67-1060

Figure 16.- Schlieren photographs showing ramjet engine simulator exhaust impinging on nozzle B2. $p_{t,X-15} = 0$.

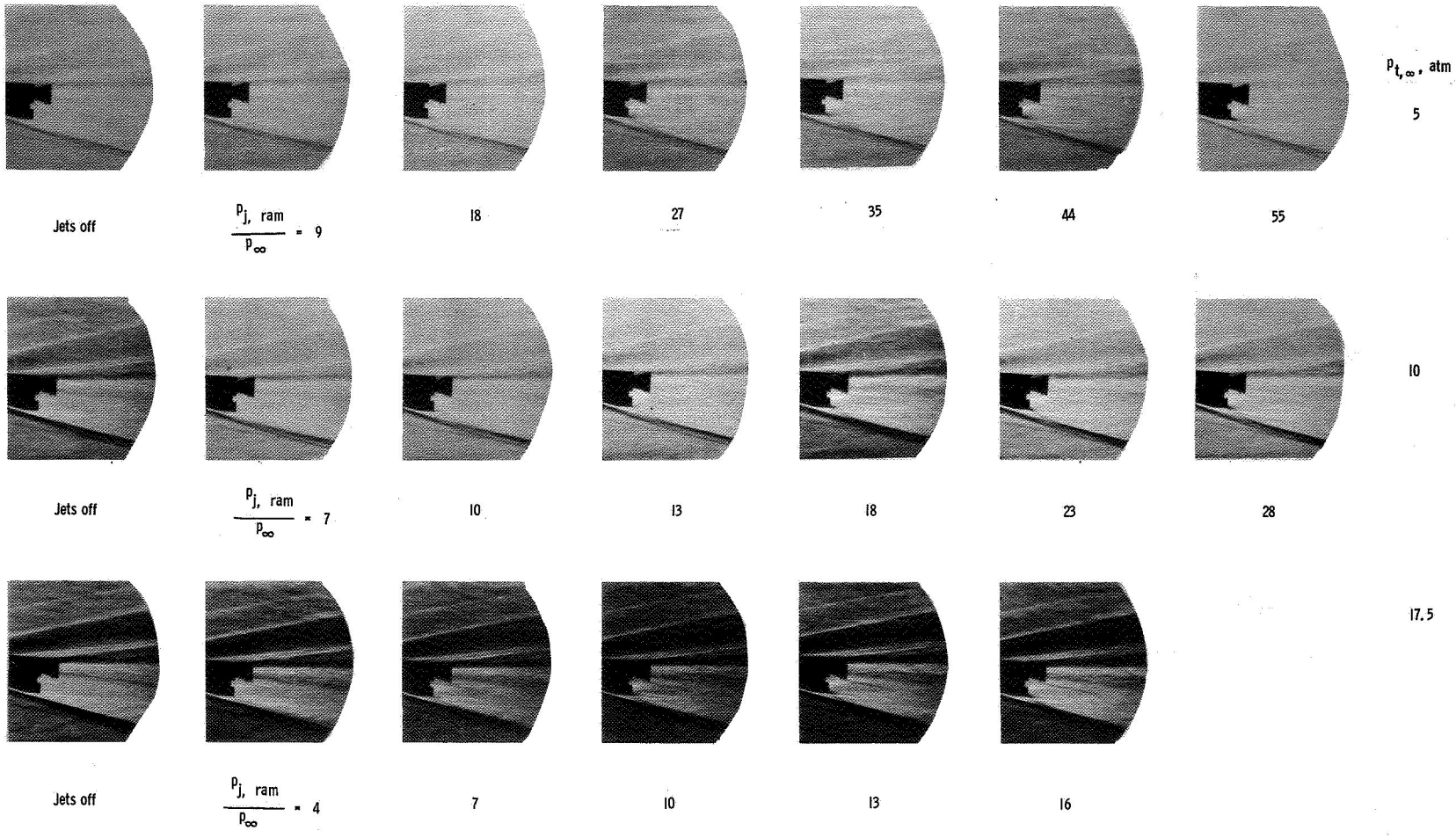

(b) $\alpha = 3^0$.

Figure 16.- Concluded.

L-67-1061

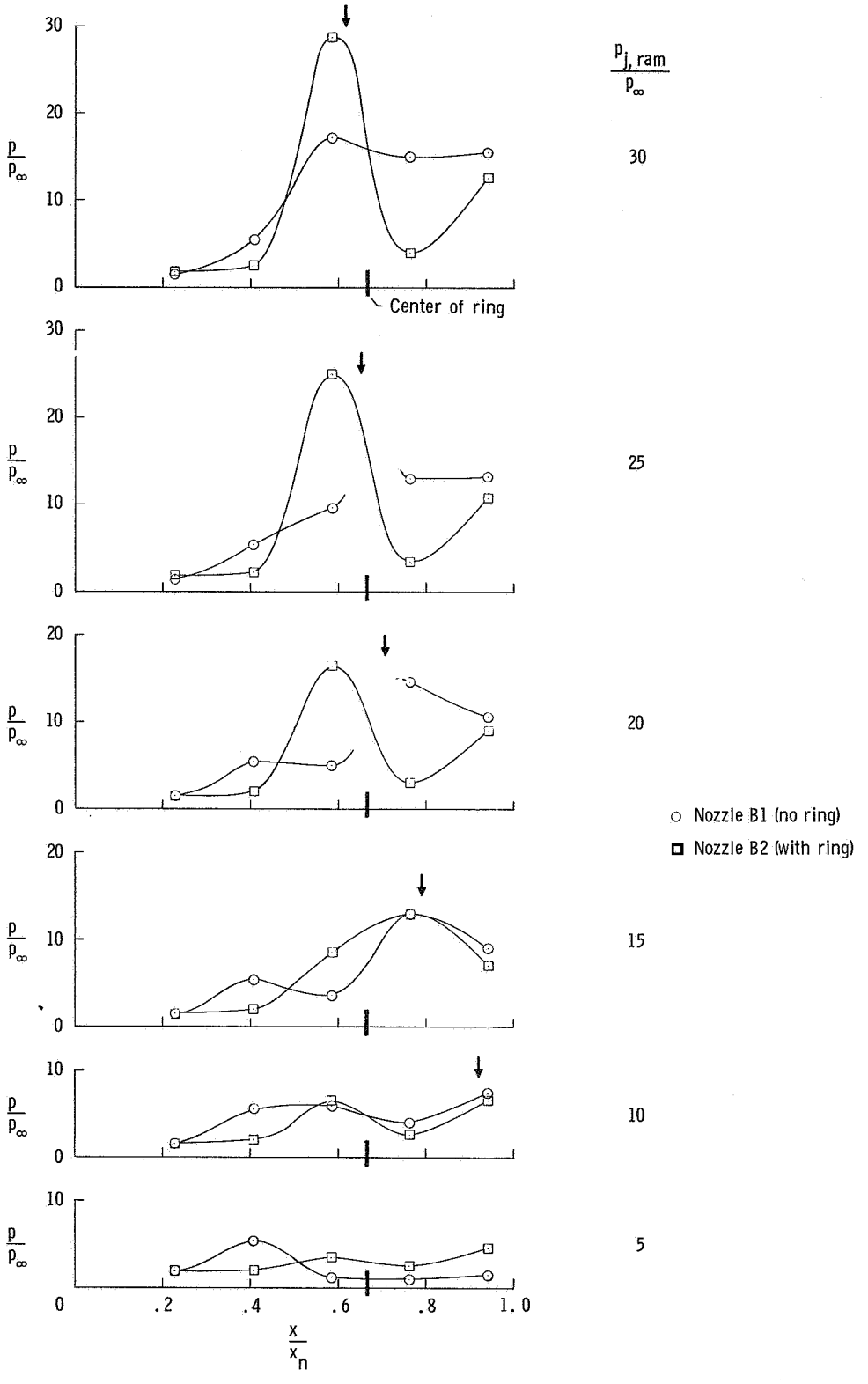

Figure 17.- Comparison of impingement effects on the external pressures of the X-15 nozzle extension with and without an attached manifold ring. $p_{t,X-15} = 0$; $\alpha = 0^0$; $p_{t,\infty} = 10$ atmospheres.

NATIONAL AERONAUTICS AND SPACE ADMINISTRATION
WASHINGTON, D.C. 20546

OFFICIAL BUSINESS

FIRST CLASS MAIL

POSTAGE AND FEES PAID
NATIONAL AERONAUTICS AN
SPACE ADMINISTRATION

POSTMASTER: If Undeliverable (Section 15
Postal Manual) Do Not Retu

"The aeronautical and space activities of the United States shall be conducted so as to contribute . . . to the expansion of human knowledge of phenomena in the atmosphere and space. The Administration shall provide for the widest practicable and appropriate dissemination of information concerning its activities and the results thereof."

—NATIONAL AERONAUTICS AND SPACE ACT OF 1958

NASA SCIENTIFIC AND TECHNICAL PUBLICATIONS

TECHNICAL REPORTS: Scientific and technical information considered important, complete, and a lasting contribution to existing knowledge.

TECHNICAL NOTES: Information less broad in scope but nevertheless of importance as a contribution to existing knowledge.

TECHNICAL MEMORANDUMS: Information receiving limited distribution because of preliminary data, security classification, or other reasons.

CONTRACTOR REPORTS: Scientific and technical information generated under a NASA contract or grant and considered an important contribution to existing knowledge.

TECHNICAL TRANSLATIONS: Information published in a foreign language considered to merit NASA distribution in English.

SPECIAL PUBLICATIONS: Information derived from or of value to NASA activities. Publications include conference proceedings, monographs, data compilations, handbooks, sourcebooks, and special bibliographies.

TECHNOLOGY UTILIZATION PUBLICATIONS: Information on technology used by NASA that may be of particular interest in commercial and other non-aerospace applications. Publications include Tech Briefs, Technology Utilization Reports and Notes, and Technology Surveys.

Details on the availability of these publications may be obtained from:

SCIENTIFIC AND TECHNICAL INFORMATION DIVISION

NATIONAL AERONAUTICS AND SPACE ADMINISTRATION

Washington, D.C. 20546